Fall 2019

Reactor configurations to support advanced material research

Thaqal Mazyad Alhuzaymi

REACTOR CONFIGURATIONS TO SUPPORT ADVANCED MATERIAL RESEARCH

by

THAQAL MAZYAD ALHUZAYMI

A DISSERTATION

Presented to the Graduate Faculty of the

MISSOURI UNIVERSITY OF SCIENCE AND TECHNOLOGY

In Partial Fulfillment of the Requirements for the Degree

DOCTOR OF PHILOSOPHY

in

NUCLEAR ENGINEERING

2019

Approved by:

Dr. Ayodeji B. Alajo, Advisor
Dr. Hyoung Lee
Dr. Carlo Castano
Dr. Xin Liu
Dr. Lana Alagha

ABSTRACT

The research goal is to configure a research reactor with multi-spectral capability for advance material research. This required the consideration of high and low-power levels alongside advanced fuel with high physical density and low enriched ^{235}U. Selected fuel was U-10Mo with 19.75% ^{235}U enrichment. The fuel and control rods system geometries were adopted from Missouri S&T Reactor (MSTR).

A high-power configuration (HPC) at 2 megawatts and low-power configuration (LPC) at 200 kilowatts were considered. Neutronic performances of the configurations were modeled using Monte Carlo N-particle (MCNP) transport code, version 6. Thermal-hydraulic analysis was performed with ANSYS Fluent. The HPC was able to support high flux levels in the order of 1E14 $n\ cm^{-2}\ s^{-1}$ with continuous operation over 2 months before refueling. The LPC provided flux between 1E12 and 1E13 $n\ cm^{-2}\ s^{-1}$ with 6 irradiation locations, which supports multiple tests at a time. The LPC fuel loading was 64% higher than the HPC.

A flexible power configuration (FPC) was developed to combine the high flux levels of the HPC and multiple irradiation facilities in the LPC. The FPC was able to replicate the neutronic performances of both LPC and HPC configurations. The FPC in low power mode sustained criticality for 2.4 years. The heat generated in high power mode was removed effectively. The calculated maximum temperatures for coolant outlet and hottest fuel plates were below the safety limits.

ACKNOWLEDGMENTS

Undertaking this Ph.D. is a giant leap towards my goals. First, I would like to thank God for everything, including the bounty, generosity, mercy, and support in all life matters.

I am indebted to my Ph.D. advisor, Dr. Ayodeji B. Alajo, for his infinite patience, tremendous efforts, and continuous support during my research. Also, I would like to thank my Ph.D. committee, Dr. Hyoung Lee, Dr. Carlo Castano, Dr. Xin Liu, and Dr. Lana Alagha, for their interest in and support of my work. Moreover, I would like to extend my sincere gratitude to Dr. Joseph Graham and Dr. Joshua Schlegel for their insightful comments and valuable suggestions.

A very special thanks to my best friend-and-brother, Meshari M. Alqahtani, for his invaluable advice and feedback. Without this continuous support, concluding this research successfully wouldn't be possible. Also, my deep appreciation goes out to my best friend, Thaar M. Aljuwaya, and all my friends for providing the continuous support and friendship that I needed.

I would like to say a heartfelt thanks to my family, especially, my mother, Katla Saqar Alhuzaymi, and brother, Zaid Mazyad Alhuzaymi. They have sacrificed their time, health, and energy for me. Words cannot express how grateful I am to my mother for her support, encouragement, prayers, and unconditional care. Also, I would like to thank my beloved and supportive wife, Ebtehal Turki Alotaibi, who provides unending inspiration during my good and bad moments. All love to my unborn son for giving me a lot of motivation and warm feelings during the concluding stage of this research.

TABLE OF CONTENTS

Page

LIST OF ILLUSTRATIONS

Figure Page

LIST OF TABLES

1. INTRODUCTION

This section provides overview of existing research reactors, describes the fuel specifications of Missouri University of Science and Technology Reactor (MSTR) and includes a discussion of the goals and motivations behind the proposed research. It also critically reviews existing research reactors in terms of current challenges, utilization, type, prevailing designs and status for advanced fuel development for research and testing reactors.

1.1. RESEARCH REACTOR OVERVIEW AND CHALLENGES

Research reactors are a very powerful tool that contribute widely to almost all of the sciences. More importantly, they are an essential element for advancing research, development and improvement in the nuclear industry, as well as other related fields [2]. Research reactors can be used for many purposes, such as training, education, isotope production and testing material behavior [2]. The primary goal of research reactors is to produce neutrons, which are beneficial for a wide range of applications such as medicine, agriculture and industry [2]. Neutrons spectrum impacts its uses [3]. Neutrons with low and intermediate energy levels (thermal and epithermal neutrons, respectively) are sufficiently produced in thermal research reactors and can be used for a wide range of purposes. These include basic irradiation experiments, neutron radiography, radiolysis, neutron activation analysis (NAA), low-scale isotope production, etc. In contrast, hard spectra are required in cases where fast neutron damage is being investigated or a high energy neutron dose is important. Experiments such as advanced tests of material behavior or large-scale isotope production can benefit from the appropriate combination of flux magnitude and energy spectrum.

One of the challenges in research reactors is the sustainment of fast neutrons in a highly moderated environment [2, 3]. Thus, some research reactors are specifically designed for the fast spectrum, including the fast flux test facility (FFTF), high flux isotope reactor (HFIR) and advance test reactor (ATR) [4–7]. However, fast research reactors are ineffective for research requiring thermal neutrons. Many experiments are focused on thermal neutrons. This is why most of the prevailing designs either focus on thermal or fast spectrum neutron [3]. Knowing that both thermal and hard spectra are needed, a combination of both spectra in a single reactor with a flexible core configuration and power level would allow for diverse irradiation experiments.

1.2. RESEARCH REACTOR UTILIZATION

Research reactors are generally categorized by their utilization [3]. It's important to note that there is no common definition for the advanced utilization of research reactors. In this work, advanced utilization of research reactor refers to the following activities: large-scale isotope production and radiation damage of materials/advanced tests of material behavior. According to the international atomic energy agency (IAEA), there are 378 research reactors worldwide [8]. Currently, 218 reactors are in operational status, 142 reactors are shutdown and 18 reactors are either under construction or planned [8]. The utilization of a research reactor depends inter alia, on its power level, and flux magnitude, along with the flux energy spectrum obtained in-core irradiation facilities [3]. The desired neutron spectrum plays a major role in designing a research reactor. The IAEA's research reactor database characterized research reactors by their power level and flux capability, see Table 1.1 [8]. Each category has specific purposes as well as advantages and limitations. For example, the low-power research reactor has a power level below kilowatt-thermal (KW-th) and a flux capability below 1E12 $n\ cm^{-2}\ s^{-1}$; therefore, it is primarily used for training and educational purposes and has limited experimental capability [8]. This type of research reactor is not suitable for advanced utilization unless the reactor core is upgraded to a higher power level.

On the other hand, a medium-power research reactor has a power level range from 1 KW-th to just below 1 megawatt-thermal (MW-th) and flux capability below 1E14 $n\ cm^{-2}\ s^{-1}$ [8]. Thus, this type has a wider scope and can be utilized for things such as neutron radiography, radiolysis, NAA, low-scale isotope production and limited tests of material behavior. However, medium-power research reactors are not suitable for a large-scale isotope production or advanced test of material behavior because such activation requires high flux capability. The only suitable type for advanced utilization is the high-power research reactor, which has a power level greater than 1 MW-th and a flux capability equal to or greater than 1E14 $n\ cm^{-2}\ s^{-1}$, see Table 1.1 [7].

Table 1.1. Categorization of Research Reactor Based on Power Level and Flux Capability.

Facility Name	Power Level (MW or KW-thermal)	Flux Capability ($n\ cm^{-2}\ s^{-1}$)	Utilization
Low-Power	<1 KW-th	<1E12	Training, education, and basic irradiation experiments.
Medium-Power	≥1 KW-th and <1 MW-th	<1E14	Training, education, neutron radiography, radiolysis, NAA, beams, low-scale isotope production and limited test of materials behavior.
High-Power	≥1 MW-th	≥1E14	Training, education, neutron radiography, radiolysis, NAA, high performance beams, large-scale isotope production and advance test of materials behavior.

Source: IAEA's Research Reactors Database [8]

1.3. TYPES OF RESEARCH REACTORS

The type of research reactor mainly depends inter alia on its design features and its planned uses [2, 3]. It should be noted that there is no international standard for characterizing or classifying types of research reactor [2, 3]. Thus, existing research reactors are categorized based on a specific design feature or a particular use. For example, a pulsed research reactor and a high-flux research reactor, were categorized based on their functionality [3]. For a pulsed research reactor, the power rises and falls quickly acting as a short pulse [3]. For a high-flux research reactor, the goal for designing such reactor is to achieve a high neutron flux inside the core in order to produce isotopes or perform irradiation damage experiments [3]. However, the most globally recognized classification of research reactor are the pool-type research reactor and tank-type research reactor [8, 9]. More details about these two types are discussed in the following subsections.

1.3.1. Pool-Type Research Reactor. The core of a pool-type reactor is near the bottom of a deep, large open-water pool. A heat exchanger is normally present at the topmost part of the pool. In most pool-type reactors, the pool water is used as a reflector and shield. However, a few pool-type reactors have solid moderator blocks that are usually made of beryllium or graphite. These blocks are placed around the active core and function as an inner reflector. In most pool-type research reactors, natural convection is used for cooling. Due to this and the radioactivity levels of water, these reactors have a limited output power. Nitrogen-16 is produced by the reaction of neutrons with the oxygen in water pool. The heat and nitrogen-16 produced in this type of reactor are directly proportional to the power of the reactor i.e. the higher the power of the reactor the more heat and nitrogen-16 are produced.

1.3.2. Tank-Type Research Reactor. Tank-type research reactors can be divided into two types: top-shielded reactors and open-tank reactors. The top-shielded reactors are mostly used for higher power levels. Open-tank reactors are mostly used for power levels around 10 MW. The arrangement of the core is like the pool-type reactors. However, the core of this type of research reactor is surrounded by solid concrete shielding. Most tank-type reactors use the forced convection cooling method due to the high generated heat inside the reactor core. Some tank-type reactors use both natural and forced convection depending on the operating power level.

1.4. PREVAILING DESIGN OF RESEARCH REACTOR

In the United States (USA), 24 research reactors are operated [8, 9]. Table 1.2 selects six of these reactors which belong to the low, medium and high-power categories. Table 1.2 contains the key characteristics of the design and capabilities of the selected reactors. The core design of these reactors varies depending on various parameters, including the type of fuel, percentage of fuel enrichment, the number of the fuel elements in the reactor core, the number of fuel plates/rods inside the fuel element, the shape of fuel the plate/rod, type of structural material used for the fuel element/plate, coolant, reflector, power level and flux capability, see Table 1.2.

MSTR, Ohio state university research reactor (OSURR), Purdue university research reactor (PUR-1) and the university of Massachusetts Lowell research reactor (UMLRR) are pool-type research reactors, while the Missouri university research reactor (MURR) and Massachusetts institute of technology reactor (MITR) are tank-type research reactors. The fuel elements of these reactors are made of Material Test Reactor (MTR) plate-type fuel, which has been licensed in many countries across the globe [2, 3]. The fuel element clads and structure use aluminum alloy due to its desirable features, such as its low thermal capture cross section. The fuel plates, either curved, or flat, or fins, contain the enriched uranium meat sandwiched by aluminum clad and placed in parallel inside the fuel element with a water channel in between. MSTR, PUR-1 and UMLRR used U_3Si_2-Al with below 20% ^{235}U enriched, see Figure 1.1. OSURR used U_3Si_2 with 19.5% ^{235}U enriched. Both MURR and MITR used UAl_x with 93% ^{235}U enriched, see Figure 1.2. A study is undergoing to convert MURR and MITR from high enriched uranium (HEU) to low enriched uranium

(LEU) [10, 11]. For each reactor mentioned, the numbers and dimensions of fuel elements and fuel plates are different depending on the design requirements. The fuel elements are arranged in a fuel element holder, usually called a grid plate, which is made of aluminum. Some positions in the fuel element holder are left empty to be used for control rods, reflectors, or experimental locations.

Table 1.2. Key Characteristic and Capability of a Specified Reactor Core Design.

Key Specification of Core Design	Reactors Name					
	MSTR	OSURR	PUR-1	UMLRR	MURR	MITR
Power Level	200 KW	500 KW	10 KW	1 MW	10 MW	6 MW
Fuel Type	U_3Si_2-Al	U_3Si_2	U_3Si_2-Al	U_3Si_2-Al	UAl_x	UAl_x
Percentage of Fuel Enrichment	19.75%	19.5%	20%	19.75%	93%	93%
Number of Fuel Elements	15	18	13	20	8	24
Number of Fuel Plate/Rod	18	16	14	18	24	15
Shape of Fuel Plate /Rod	Curved	Flat	Flat	Flat	Curved	Flat + Fins
Coolant	H_2O	H_2O	H_2O	H_2O	H_2O	H_2O
Reflector	H_2O/ Graphite	H_2O/ Graphite	H_2O/ Graphite	H_2O/ Graphite	Beryllium/ Graphite	Heavy Water/ Graphite
Highest Neutron Flux ($n\ cm^{-2}\ s^{-1}$)	4.36 x 10^{12}	In the range of 10^{12} – 10^{13}	2.1 x 10^{10}	In the range of 10^{12} – 10^{13}	6.0 x 10^{14}	1.2 x 10^{14}

Source: References number [10–16]

The previously mentioned cores are cooled by either natural convection or forced convection depending on the generated heat and power level. UMLRR, MURR and MITR used both natural and forced convection for cooling. In most of the open pool-type research reactors, water serves as the moderator, reflector, shielding, and heat removal medium. As a reflector, water and graphite have been used, except for MURR and MITR where they used beryllium/graphite and heavy water/graphite, respectively. Along with all of the

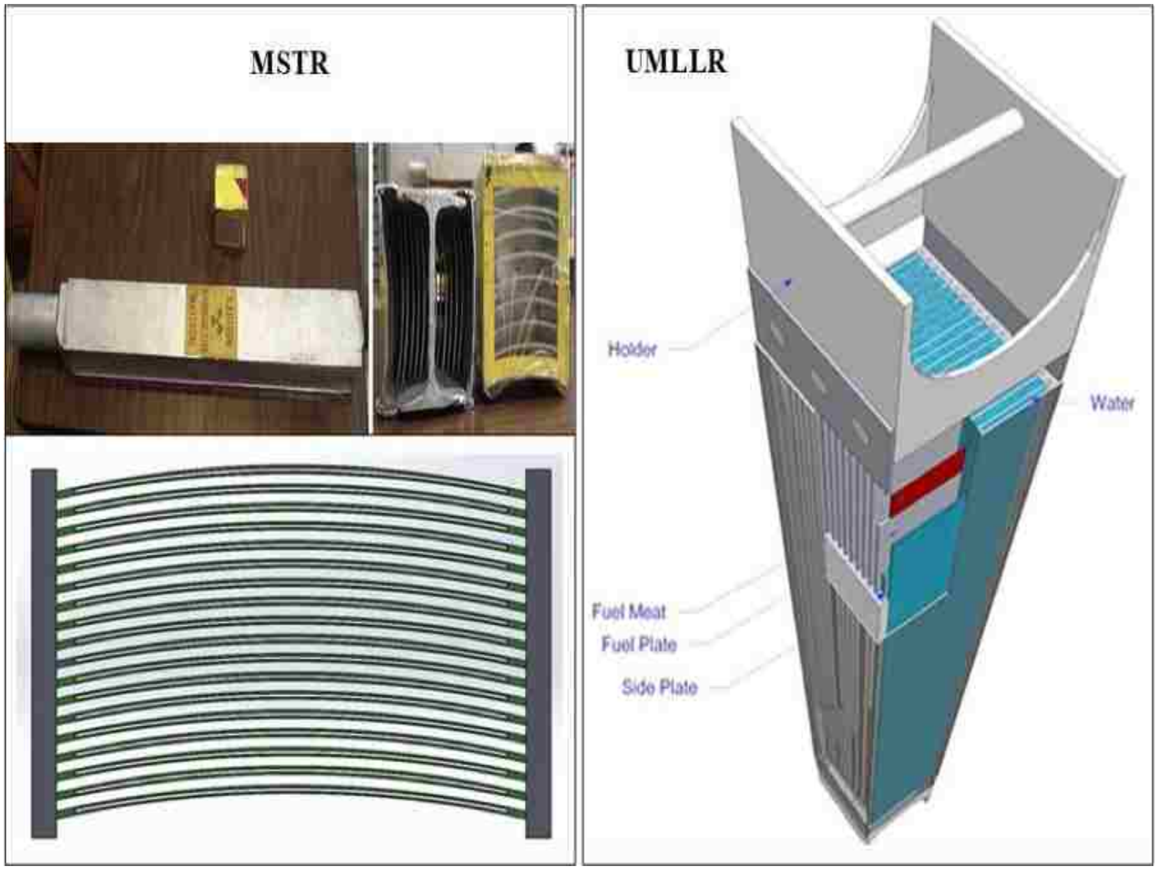

Figure 1.1. Fuel Element for MSTR and UMLRR.

variation in the design of components for the reactors mentioned previously, power level and flux capability, inter alia, contributed significantly to shaping the reactors' activities and capabilities. Most of these reactors have a flux capability ranging in the order of 10^{10} to 10^{13} $n\ cm^{-2}\ s^{-1}$ except for MURR and MITR which have flux capability in ordered of 10^{14} $n\ cm^{-2}\ s^{-1}$.

1.5. SAFEGUARD AND NONPROLIFERATION IN RESEARCH REACTOR

From safeguard and nonproliferation point of view, nuclear facility containing high-enriched uranium (HEU) fuel are identified as a potential threat for diversion, sabotage and misuse of sensitive nuclear materials or a weapon-usable material [17, 18]. In research-

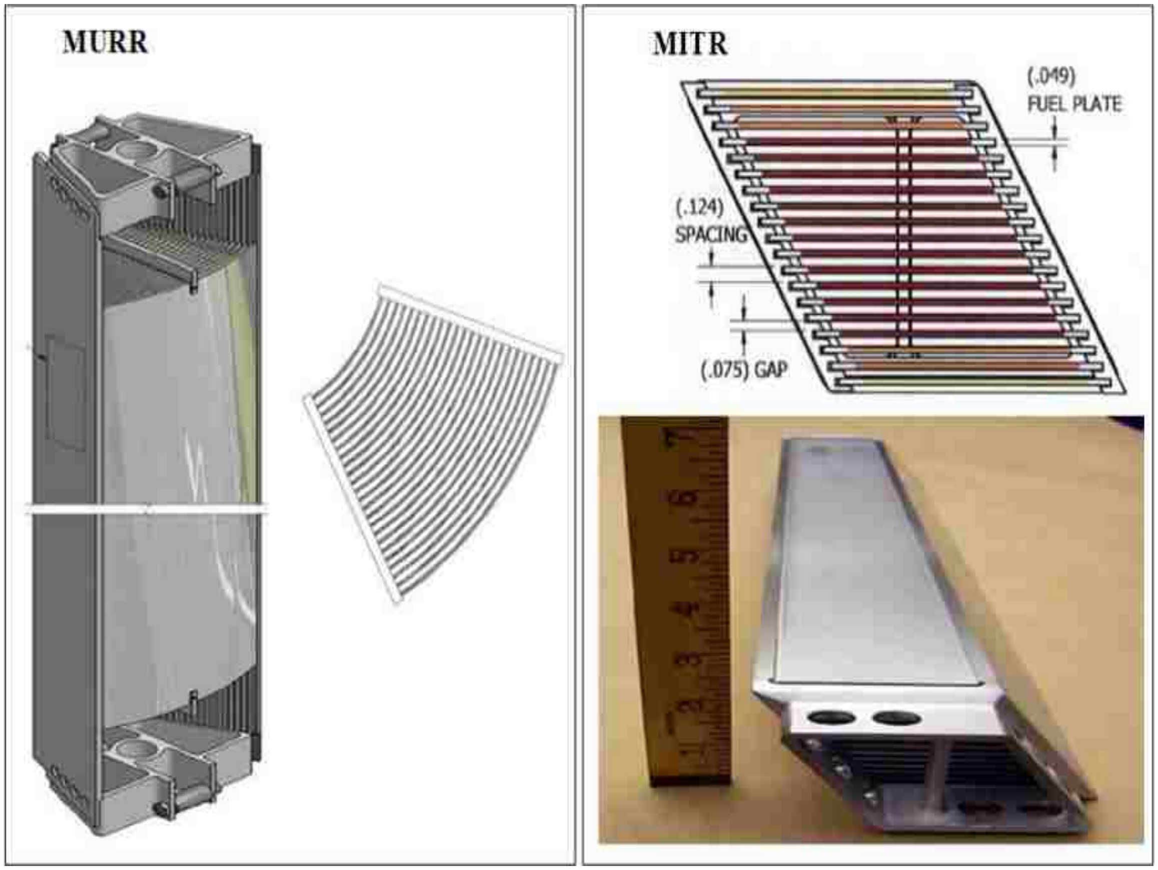

Figure 1.2. Fuel Element for MURR and MITRR.

reactors community, many of high-power research reactors, testing or isotopes production facilities used HEU fuel [17, 18]. To prevent the diversion, sabotage and misuse of sensitive nuclear materials, global threat reduction initiative (GTRI) has undertaken several initiatives for quantifying, qualifying, developing, fabricating and manufacturing a LEU fuel for high-power research reactors and testing facilities. One of these initiatives is the conversion initiative, which aims to convert the existing civilian isotope production facilities and testing research reactors in USA from HEU fuel to LEU fuel. The development and deployment of a new LEU fuel was undertaken by the Reduced Enrichment for Research Test Reactor (RERTR) program which started in 1978 by the Argonne National Laboratory (ANL).

In 2015, Material Management and Minimization (3M) was established to continue the previous effort of GTRI with a wider scope. The goal of 3M conversion program is to minimize and eliminate the use of HEU fuel worldwide, as explained in [19]. "The primary objectives of 3M is to achieve permanent threat reduction by minimizing and, when possible, eliminating weapons-usable nuclear material around the world". 3M conversion program targeted high-power research reactors or testing facilities in USA and around the world. The targeted facilities in USA included HFIR, MURR, MITR, the national bureau of standard reactor (NBSR) the advanced test reactor (ATR) and the advanced test reactor-critical facility (ATRC) [17]. These reactors considered all possible efforts to convert from HEU fuel to LEU fuel [1, 17, 18]. The conversion efforts involved adopting advanced LEU fuel, modifying the designs of core elements, increasing the power level of the reactor, evaluating the fuel load in-core and many others [1, 17, 18]. Globally a couple of research reactors with HEU fuel were converted to LEU fuel with the support of 3M conversion program and international community lead by IAEA [1, 17, 18]. For example, the Ahmadu Bello University Research Reactor (ABU RR) in Zaria, Nigeria successfully converted its core from HEU fuel to LEU fuel in 2018 [20]. In line with the previously mentioned efforts and to eliminate the potential threat of misusing sensitive nuclear materials, new design of research reactors should consider the LEU fuel along with minimizing, as much as possible, the load of fuel in-core.

1.6. ADVANCED FUEL DEVELOPMENT FOR RESEARCH REACTORS

Uranium silicide-aluminum dispersion fuel (U_3Si_2-Al) is widely used for low and medium-power research reactors. U_3Si_2-Al fuel used with 19.75% ^{235}U enriched and low physical density [12, 17, 21]. However, it is not a preferable option for testing research reactor or for high-power upgrading purposes [1, 17]. This is due to the low physical density of fuel (~5.5 g/cm^3) associated with the low enrichment (19.75% ^{235}U enriched) [1, 12]. This fuel will be insufficient in providing the desired performance such as reactivity, neutron flux and burnup [1, 17]. More importantly, maintaining core criticality with respect to the core configuration will be difficult to achieve [1, 17]. Because of these reasons, this section provides an overview of the current status of LEU fuel development by RERTR conversion program for research and testing reactors.

Characterization of research reactor fuels relies on many parameters including the geometrical shape of the fuel, cladding material and most importantly the embedded fuel structural material [1, 17, 18, 21]. From a geomaterial point of view, most of the testing research reactors in the USA used plate-type fuel, either in flat or curved shape [1, 17, 18, 21]. Fuel is usually clad by aluminum alloy or aluminum, most commonly 6061 Al [1, 17, 18, 21]. Dispersion fuels are widely used for MTR plate-type fuel [3–5]. Dispersion fuel comes in the form of ceramic triuranium octaoxide (U_3O_8) or intermetallic uranium aluminide (UAl_x). Table 1.3 summarizes the general fuel classification for most of the existing high-power research reactors in the USA [1, 17, 18, 21]. Fuel comes in three chemical forms: alloy, ceramic and intermetallic which can be fabricated as a monolith or dispersed in a matrix, creating its physical form, see Table 1.3. Dispersion fuel exists in powder form containing the fuel materials in a metallic matrix [1, 17, 18, 21]. Monolith fuel consists of a continuous medium and is commonly called “fuel meat” [1, 17, 18, 21]. Cermet fuel is an intermetallic fuel or ceramic in dispersion form. For commercial power reactors, the porosity of the dispersion fuel provides gaps between fuel and clad which allows for the accumulation of helium and fission gas along with reducing fuel swelling. For the MTR plate-type fuel, no such gap exists between fuel and clad [1, 17, 18, 21]. In contrast, monolithic fuels allow for higher levels of physical density and higher melting points [1, 17, 18, 21]. Therefore, monolithic fuel has been widely used for testing research reactors. Another fuel that was not included in Table 1.3 is caramel fuel, which comes with no interstitial matrix and consist of a miniature uranium oxide [1]. Even though it allows for high physical density and accommodates fission gas buildup, it was not considered by the RERTR program

[1, 17, 18, 21]. Caramel fuel is not used by the previously mentioned high-power research reactors in USA. France used caramel fuel in some if its reactors and led the development of the caramel fuel [1].

Table 1.3. Fuel Classification for High-power Research Reactors [1]

Chemical Form	Physical Form	Examples	Comments
ALLOY	Monolithic	U-Al, U-Mo, U-Z_r, U-Z_rH_x	High physical density of material, high κ
	Dispersion	U-Mo-Al	Matric allows for fission gas accumulation
CERAMIC	Monolithic	UO_2	High melting point, Good temperature stability
	Dispersion	U_3O_8-Al	"Cermet" fuel, Advantages of ceramic with better bulk κ
INTERMETALLIC	Monolithic	U_3Si_x	Very high uranium loading achievable
	Dispersion	UAl_x-Al, U_3Si_x-Al	"Cermet" fuel, Good mix of properties, porosity allows for fission gas accumulation

Source: Eric C. Forrest, Dissertation, 2014[1]

Alloy fuel is widely used for high-power research reactors [1, 17, 18, 21]. ATR, ATRC, MURR and MITR used UAl_x fuel, which has a low physical density but a very high enrichment (93% ^{235}U enriched) [17]. The very high enrichment employed to overcome the low physical density of alloy. Therefore, fuel allow providing the desired performance. For fuel conversion to LEU, the RERTR program studied varying candidate fuels such as UO_2, U_3O_8, UAl_x and others [1, 17, 18, 21]. The selection for the best available candidate fuel was uranium-10 wt% molybdenum metallic alloy (U-10Mo) with 19.75% ^{235}U enriched [1, 17, 18, 21]. Table 1.4 presents U-10Mo physical properties compared to some of the other candidate fuels. Comprehensive details about all candidate fuels can be found in [1, 17, 18]. The reasons behind the selection of U-10Mo are the very high uranium density (theoretical density of 17.2 g/cm^3), stability and predictable irradiation behavior [1, 17, 18, 21]. Due to the undesired reaction between the aluminum and U-10Mo foil and to avoid delamination and blistering, a diffusion barrier is required [1, 17, 18, 21]. Reaction between aluminum and U-10Mo foil could cause swelling in case of high burnup and fission rate [17]. Experimental evaluation of U-10Mo fuel demonstrated the occurrence of delamination and blistering in cases of high temperature environment [22]. Thus, RERTR proposed a thin zirconium layer 25.4 m-thick (1 mil) to surround the fuel meat, acting as diffusion barrier [1, 17, 18, 21]. However, the issue that has delayed the availability of U-10Mo fuel is the ability of aluminum clad to accommodate fission gas buildup in a plate-type fuel [1, 17, 18, 21]. Today, U-10Mo fuel is under development and qualification [1, 17, 18, 21]. MITR, MURR and ATR have carried out neutronic and thermohydraulic studies for the consideration of U-10Mo fuel [23–25].

Table 1.4. Physical Properties for Some of the Candidate Advanced Fuel Materials [1]

	$T_{melt}(C^0)$	Theor. Density (g/cm^3)	Current U Loading[g]/Max. U Loading (gU/cm^3)	Physical Form[e]	κ (w/m-k)	c_p (J/kg-k)	Thermal Expansion Doff. (k^{-1})	Yield Strength [a](MPa)	Status
UAl_x in Al:		6.4	2.3/2.8						In use-research and test reactor fuel.
UAl_2	1688	8.1		FCC					
UAl_3	1349	6.7		SC					
UAl_4	732	6.0		O					
U_3O_8 in Al	1300[f]	8.40	3.2/3.8	O	18				In use- research and test reactor fuel.
UO_2	2875	10.96	9.1/9.1	FCC	~ 10				In use as LWR fuel.
U_3Si_2 in Al	1665	12.2	4.8/6.0		~ 50				Qualified and approved by US NRC.
U-10Mo	1150	17.1	16.38	$\alpha+\delta$ phase[d] (O+T)	~ 17.6	142	1.23×10^{-5}	933 (γ-quench)	Prior use in research reactor. Under development for test reactor.

Source: Eric C. Forrest, Dissertation, 2014[1]

[a] Yield strength is for annealed specimens, unless otherwise noted.

[d] Metastable in -phase (BCC) with appropriate quenching heat treatment.

[e] FCC=Face Centered Cubic; HCP=Hexagonal Close Packed; O=Orthorhombic; SC=Simple Cubic; T=Tetragonal

[f] Decomposes.

[g] Current achievable uranium loadings for UAl_x-Al, and U_3O_8-Al were developed and qualified under RERTR.

1.7. GOAL AND OBJECTIVES

The goal of this study is to overcome the attendant rigidity of the traditional design of research reactor and provide adaptability and flexibility in supporting a wide variety of experiments and research. This can be achieved by investigating a conceptual core design and configuration. For the conceptual design, the fuel and control rods system geometries were adopted from MSTR. The conceptual investigation included neutronic and thermal-hydraulic evaluations. The neutronic evaluation involves core criticality calculation, determination of the neutron flux profile over the core and flux spectrum determination in-core irradiation facilities, control rod worth and safety shutdown margin, burnup analysis and other aspects related to characterizing the core's neutronic performance. The conceptual investigation comes with inevitable key considerations especially in terms of thermal-hydraulic behavior: for example, heat removal and cooling requirements. For the sake of thorough investigation, the thermal-hydraulic performance was evaluated. More details about the neutronic and thermal-hydraulic evaluations will be discussed in the body of this study.

The objectives behind the conceptual design and configuration are; 1) the achievement of high neutron flux inside in-core irradiation facilities and 2) adaptability and flexibility in core configuration and power level. The adaptability and flexibility will allow the core to be configured for both high-power mode and low-power mode. In other words, configuring core for high-power applications and low-power applications. By shuffling the reactor core components around the core along with adjusting the reactor power level, the user would be able to shift from low-power mode to high-power mode. For the high-power mode, neutronic and thermal-hydraulic aspects will be both evaluated. For the low-power mode, only neutronic aspects will be evaluated. Due to the low power level of the reactor for the low-power mode, natural convection was assumed to be sufficient for removing the heat generated inside the reactor core.

1.8. TASKS AND KEY FEATURES

The tasks for the proposed study involve characterizing the reactor core performance from a neutronic and safety perspective. The neutronics evaluation will be performed using the Monte Carlo N-particle (MCNP) transport code. The MCNP code is a physics-rich Fortran90 computer code that was designed by the Los Alamos National Laboratory (LANL) during the 1940s, modeling the interaction of radiation with matter [26]. A thermal-hydraulic evaluation will be performed using computational fluid dynamic (CFD) codes and first principle calculation where applicable. The CFD codes are a well-known computer tool for solving thermal-hydraulic problems [27]. The involved tasks can be characterized and listed as follows:

1. Designing and configuring the reactor core for high-power configuration (HPC) and low-power configuration (LPC);
   - Configurations were combined in flexible-power configuration (FPC), which can operate at high and low-power levels.
2. Defining various parameters and metrics in the reactor core for the quantification of its performance.
3. Characterizing the reactor core for heat removal strategies for high-power level.

One of the key features for this study is to have a research reactor with flexibility on core configuration and power level. The flexibility in power coupled with core configuration would optimize neutron fluxes in the reactor core. Two power levels would be considered, including high-power and low-power levels. The power level for high-power configuration (HPC) is 2 MW and 200 KW for low-power configuration (LPC). The HPC provides capabilities inherent to medium and high-powered research reactors. The LPC provides the capability for steady-state criticality experiments, where limited to no reactivity feedback is desired. Flexible-power configuration (FPC) was proposed to combine the advantages of both HPC and LPC configurations. FPC considered operating at both high-power level (2 MW) and low-power level (200 KW).

Another key feature for this study is to have a research reactor with a multi-spectral capability. This can be achieved by the inclusion of multiple in-core irradiation facilities. The configuration of the reactor core would include several features, such as the inclusion of a flux trap (FT) facility at the central region of the reactor core. The flux trap concept concentrates and enhances the flux in a specific location in the reactor core. Furthermore, a centrally located FT takes advantage of the higher neutron population at this location compared with other locations in the reactor core. Other configuration features include the placement or location of other in-core irradiation facilities (for example, HC, BRT and CRT). The location of the included irradiation facilities significantly impacts its performance. With respect to all the involved parameters of the reactor core design, the in-core irradiation facilities would be strategically located to optimize core neutronics performance.

Another key feature of this study is the heat removal strategy. Most of the thermal research reactors produce a relatively small amount of heat, especially for those with low-power levels. For the low-power mode, natural convection of the pool water was assumed to be adequate for heat removal. Moreover, for the high-power mode, a thermal-hydraulic evaluation is required to determine the adequacy of natural convection for heat removal or the need for forced circulation.

1.9. DESCRIPTION OF MSTR FUEL AND CONTROL ROD SYSTEM

MSTR is an open pool-type research reactor used for training and educating nuclear engineering students along with conducting experiments and research [12]. The research conducted included neutron activation analysis (NAA), neutron radiography, radiolysis and image processing. The MSTR operates at up to 200 kilowatt (kW) [13]. Light-water is used for moderation and natural convective heat removal [13]. The MTR plate-type fuel is used.

	1	2	3	4	5	6	7	8	9
A									
B						**S**			
C					**CR4**	**FE**	**FE**	**FE**	
D				**FE**	**FE**	**FE**	**CR1**	**FE**	**FE**
E				**FE**	**CR3**	**FE**	**CR2**	**FE**	**FE**
F				**CRT**	**FE**	**HC**	**FE**	**BRT**	**FE**

S: Source Holder FE: Fuel Element CR#: Control Rod
HC: Hot Cell BRT: Bare Rabbit Tube CRT: Cadmium Rabbit Tube

Figure 1.3. MSTR Current Core Configuration, called “120W” configuration.

The grid plate is a nine by six aluminum array containing about 54 positions [12]. The core consists of nineteen fuel elements and three in-core irradiation facilities along with the one source holder [12]. The current MSTR core configuration is presented in Figure 1.3 and is the so-called “120W” configuration. Four of the fuel elements are used for reactor power control (control rods) and are positioned at C5, D7, E5 and E7, see Figure 1.3.

The fuel element is 87 cm tall and has a cross-sectional area of 7.62 x 7.62 *cm*, see Figure 1.4(A). The bottom of the fuel element has a cylindrical nose piece, which helps plug it to the grid plate. Each of the fuel elements consist of eighteen curved fuel plates, which are comprised of U_3Si_2-Al [13]. The fuel plate is filled with 12.5 *g* of uranium enriched to 19.75% ^{235}U [13]. The fuel plate has two regions: fuel meat “U_3Si_2-Al” and aluminum clad. The overall thickness of the fuel plate is 0.13 *cm* [13]. The fuel meat and cladding thickness are 0.05 *cm* and 0.0395 *cm*, respectively [13]. The water cap thickness between fuel plates is 0.31 *cm* [13]. The four elements used for reactor power control (control

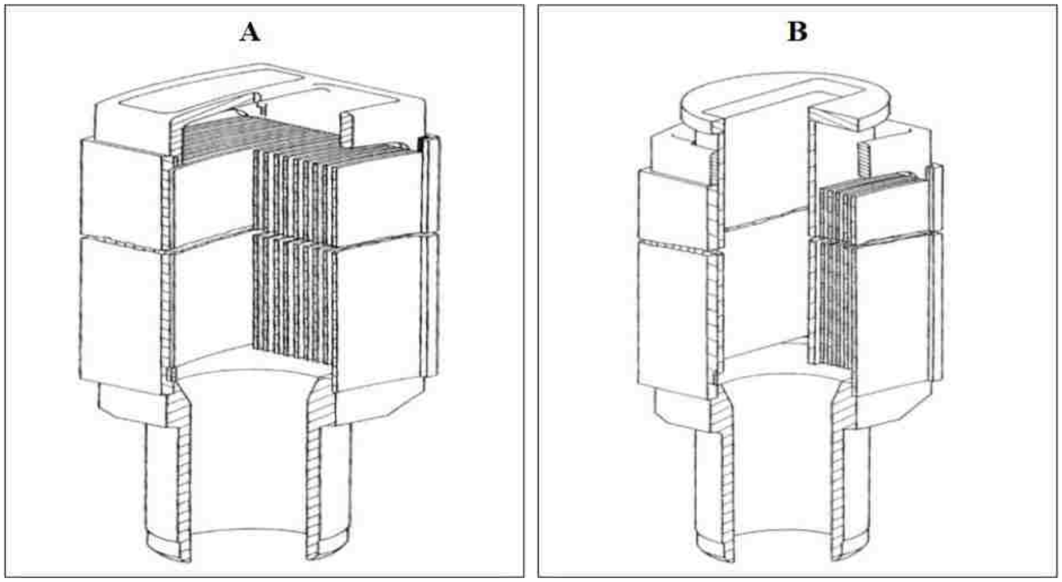

Figure 1.4. Standard Fuel Element-A and Control Rod-B.

rods) are the same as the design of the standard fuel element, except the eight middle fuel plates were removed to accommodate the control rod insertion (control rod channel), see Figure 1.4(B). Three of these are shim-safety rods, which are made of 1.5% natural-boron stainless steel [12, 13]. The fourth one is the regulating rod, which is made of SS304 stainless steel [12, 13].

2. THE PROPOSED HIGH-POWER CONFIGURATION (HPC)

The goal of the proposed high-power configuration (HPC) is the achievement of high neutron flux to support advance experiments and researches. The current MSTR features served as the basis for HPC. HPC involves modifying features to be able to achieve the desired goal. Theses modified features includes; 1) changing the type of fuel meat, 2) modifying the design of fuel plates, 3) inclusion of flux trap facility, 4) configuration of the reactor core to adopt a compact core concept and 5) increasing the boron concentration in control rods system for an effective shutdown. The adopted power level for HPC was 2 MW. The magnitude of neutron flux is linearly proportional to the reactor power [17, 28]. Therefore, increasing the power level will yield a proportional increase in the neutron flux. In the process of converting MURR and MITR fuels from HEU to LEU, both reactors considered the possibility of uprating power levels to compensate the neutron flux losses [17]. However, uprating the power level impose re-evaluating the reactor thermal-hydraulic behavior.

The current MSTR fuel is not a preferable option for HPC due to the low physical density of fuel (5.5 g/cm^3) associated with the low enrichment (19.75% ^{235}U enriched) [12, 13]. It will be insufficient in providing the desired performance such as reactivity, neutron flux and burnup [1]. More importantly, maintaining core criticality with respect to the core configuration will be difficult [1]. The U.S. high-power research reactor such as MITR, MURR and ATR used UAl_x fuel which has low physical density (~ 3.6 g/cm^3) but a very high enrichment (93% ^{235}U enriched) [1, 7, 17]. The high enrichment was employed to overcome the low physical density of alloy in order to achieve the desired performance [1]. For fuel conversion to LEU, the reduced enrichment for research test reactor (RERTR) program, selected uranium-10 wt% molybdenum metallic alloy (U-10Mo) with 19.75% ^{235}U enriched to be the best candidate fuel [1, 17, 23–25]. The reasons behind the selection of U-10Mo are due to its very high uranium density (16.09 g/cm^3), stability and predictable irradiation behavior [1, 17, 23–25]. However, due to the undesired reaction between the aluminum and U-10Mo foil and to avoid delamination and blistering, a diffusion barrier is required [1, 17, 23–25]. Reaction between aluminum and U-10Mo foil could cause swelling in case of high burnup and fission rate [17]. Experimental evaluation of U-10Mo fuel demonstrated the occurrence of delamination and blistering in case of a high temperature environment [22]. Thus, RERTR proposed a thin zirconium layer of 25.4 μm-thick (1 mil) to surround the fuel meat acting as diffusion barrier [1, 17, 23–25]. However, the issue that's delayed the availability of U-10Mo is the ability of aluminum clad to accommodate fission gas buildup in a plate-type fuel [1, 17]. Till today, U-10Mo fuel is under development and qualification. MITR, MURR and ATR performed a neutronic and thermohydraulic studies for the consideration of U-10Mo fuel [23–25]. Therefore, U-10Mo fuel is the best available candidate to be considered for HPC. The current MSTR fuel plate is modified to accommodate the consideration of U-10Mo with a thin zirconium layer, see Figure 2.1 [28].

Third modified feature for HPC is the inclusion of a flux trap (FT) facility to be positioned at the central region of the reactor core [28]. The flux trap concept facilitates concentration and enhancement of neutron flux in a specified region. A centrally located FT takes advantage of the higher neutron population. The FT design is a cylinder with a radius of 3.2 *cm*, 60 *cm* tall and placed inside an empty standard fuel element shell. Other in-core irradiation facilities considered for HPC is BRT and CRT. The design and geometry of both BRT and CRT remain unchanged, as it's in the current MSTR core [28].

Forth modified feature for HPC is the configuration of the reactor core to adopt compact core concept, see Figure 2.2 [28]. The grid plate modified to 9x9 aluminum array which allow 81 positions. The HPC core contains four fuel elements, four control rods and three irradiation facilities namely, FT, BRT and CRT, see Figure 2.2 The core is surrounded by a graphite blocks for neutron reflection purpose and to help maintaining critical core. The graphite block is an empty standard fuel element shell that filled with graphite. The

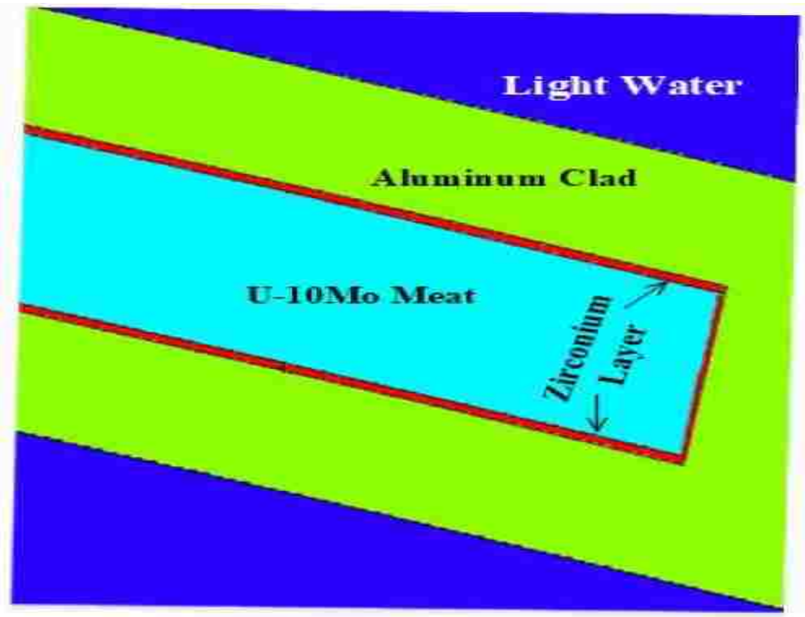

Figure 2.1. Middle-Cut-View of a single fuel plate containing U-10Mo Meat surrounded by thin zirconium layer, aluminum clad and light water.

strategy behind selecting graphite is due to its affordability and the well-known behavior as reflector material. Beryllium Oxide (BeO) is another material that can be consider as a reflector. Both materials have been in-use for research and power reactors however, BeO is expensive in comparison to graphite [29–31]. In contrast, BeO is a better neutron reflector due to its unique features, for example scattering and thermal absorption cross-section [32–34]. Thus, HPC initially considered a reflector block fully filled with graphite. In addition, an introduction of a thin BeO slab (0.5 *cm*) to the reflector block was studied in term of neutronic effects, broader details will be provided in the results section. The fuels are contained in the central 3x3 grid (D4:F6), see Figure 2.2. Fifth modified feature for HPC is increasing the boron concentration in control rods to 2% for an effective safety shutdown [28].

	1	2	3	4	5	6	7	8	9
A									
B						GB			
C			GB	GB	GB	BRT	GB		
D			GB	FE	CR1	FE	GB		
E			GB	CR4	FT	CR3	GB		
F			GB	FE	CR2	FE	GB		
G			GB	GB	GB	CRT	GB		
H						GB			
L									

GB: Graphite Block FE: Fuel Element CR#: Control Rod
BRT: Bare Rabbit Tube CRT: Cadmium Rabbit Tube FT: Flux Trap

Figure 2.2. HPC Core Configuration.

2.1. MCNP MODEL AND SIMULATION CONDITIONS

An existing high-fidelity MCNP model of the MSTR facility was modified to represent the proposed HPC. The fuel plate models were modified to accommodates the U-10Mo fuel with a thin zirconium layer. The total thickness of the curved fuel plate remained unchanged (0.13 *cm*) where the zirconium thickness was subtracted from the original cladding thickness which was 0.0395 *cm*. Therefore, the new cladding thickness is 0.0392 *cm* in each sides of the fuel meat. The fuel plate dimensions for both of HPC and the current MSTR is compared in Table 2.1. Other modifications to MSTR original MCNP model were, 1) change of grid plate to 9x9 aluminum array, 2) repositioning four fuel elements, 3) repositioning four CRs; three of which are shim-safety rods and one regulating rod, 4) inclusion of the previously described FT, 5) repositioning BRT and CRT and 6) inclusion of block reflectors around the core.

Table 2.1. Dimensions Comparison of Fuel Plate for Current MSTR and HPC.

	Current MSTR	HPC
Width of Fuel Meat	0.051 *cm*	0.051 *cm*
Length of Fuel Meat	61 *cm*	61 *cm*
Thickness of Clad	0.0395 *cm*	0.039246 *cm*
Thickness of Zirconium	-	0.000254 *cm*
Total Thickness of Fuel Plate	0.13 *cm*	0.13 *cm*
Water Gap Between Plates	0.31 *cm*	0.31 *cm*

By including all the necessary modifications for HPCs' MCNP model, a number of tasks were identified for performing the simulation. The identified tasks were listed as following:

1. Determination of neutron multiplication factor (k_{eff}).
2. Analyzing the optimum BeO to graphite thickness ratio.
3. Determination of CRs safety shutdown margin.
4. Determination of neutron flux map over HPC core and neutron flux spectrum in-core irradiation facilities.
5. Burnup analysis.
6. Determination of hot-channel for both clean and burned cores.

For determining k_{eff} "excess reactivity", all control rods were fully withdrawn and a KCODE criticality calculation was set up using 20000 particles per cycle, 300 active cycles, and 20 discarded cycles. A mesh card was set up over the actual geometry of the core for flux map determination at full power (2 MW). Tally F4:N was used for determining flux spectrum in-core irradiation facilities at a full power. For the cross-section data library, ENDF/B-VI was used for all isotopes in the model. In addition, temperature card was used to modify cross-section to the expected operation temperature. For HPC core the estimated operation temperature was 341.12 k. For burnup analysis, a burnup card was included in the MCNP model and set up for determining how long the reactor core can support sustained criticality. For hot-channel determination at 2 MW, a single mesh was created for each fuel plates in the core (core contains 112 fuel plates) to track fission energy deposition. All simulations were performed using MCNP version 6 [26].

2.2. RESULTS AND DISCUSSION

This section included an evaluation of four different fuels, control rod worth and safety shutdown margin, analysis of the optimum thickness ratio of composite reflector blocks containing BeO and graphite, determination of flux map and spectrum, and evaluation of HPCs' potential operation time.

2.2.1. Comparison of Different Fuel for HPC Core. Four different fuel were evaluated for HPC core, see Table 2.2. 19.75% U-235 enriched was considered for all the evaluated fuels. UO_2 is a ceramic fuel with a theoretical density of 10.96 g/cm^3 [35]. Also, it has the advantages of high melting point (2875 ^{0}C) and good temperature stability. It has long history for being used for light water reactors (LWR) worldwide. U_3Si_2-Al is intermetallic fuel with a theoretical density of 12.2 g/cm^3 [1]. It has been widely used for low and medium research reactor. U_3Si_2-Al has high melting point (1665 ^{0}C) and thermal conductivity of 50 W/m K [1]. UAl_x is also intermetallic fuel with theoretical density up to 8.1 g/cm^3 for UAl_2 [17]. It has melting point of 1400 ^{0}C and thermal conductivity of 42.5 W/m K [1]. Mostly used for testing reactor but with high enrichment (93%) [10, 11]. U-10Mo is metallic fuel with high theoretical density (17.2 g/cm^3) [17]. It was used (with 26% U-235 enriched) for the first time in 1963 by Enrico Fermi Fast Breeder reactor [1]. It has high melting point (1150 ^{0}C) with thermal conductivity of 17.6 W/m K. U-10Mo fuel allows for high physical density compared to other candidate fuels. By employing all the evaluated fuels in the HPC core, only U-10Mo allow for critical core, see Table 2.2. The k_{eff} determination was evaluated in a room temperature along with the control rods fully withdrawn and the reflector blocks were fully filled with graphite. Even with considering the maximum theoretical density for each fuel, a critical core cannot be sustained except with U-10Mo. For U-10Mo, the determined k_{eff} was 1.02239 with an estimated standard deviation of 0.00036.

Table 2.2. Comparison of Different fuel for HPC Core.

Fuel Type	UO_2	U_3Si_2-Al	UAl_x	U-10Mo
Fuel Form	Ceramic	Intermetallic	Intermetallic	Metallic
Fuel Thermal Conductivity(W/m K)	~10	50	42.5	17.6
Melting Point (^{0}C)	2875	1665	~1400	1150
Fuel Density (g/cm^3)	10.41	5.52	3.88	16.09
HPC Core Configuration				
Multiplication Factor (k_{eff})	0.98760	0.81878	0.80746	1.02239
Estimated Standard Deviation	0.00038	0.00028	0.00033	0.00036

2.2.2. Control Rod Worth and Safety Shutdown Margin. For the determination of safety shutdown margin, two pair of control rods are assumed to be the shutdown control rods, the third is the extra shutdown control rod and the fourth is the regulating control rod. The pair of shutdown control rods are tested in all of four control rods positions namely, D5-(CR1), E4-(CR4), E6-(CR3) and F5-(CR2), see Figure 2.2. The effective pair of shutdown control rods are determined to be in the position of CR1 and CR2. With a full insertion of CR1 and CR2, k_{eff} is 0.93395 with an estimated standard deviation of 0.00037. The worth of pair shutdown control rods (CR1&2) are plotted in Figure 2.3. CR4 was assigned to be the extra shutdown control rod and CR3 was assigned to be the regulating rod.

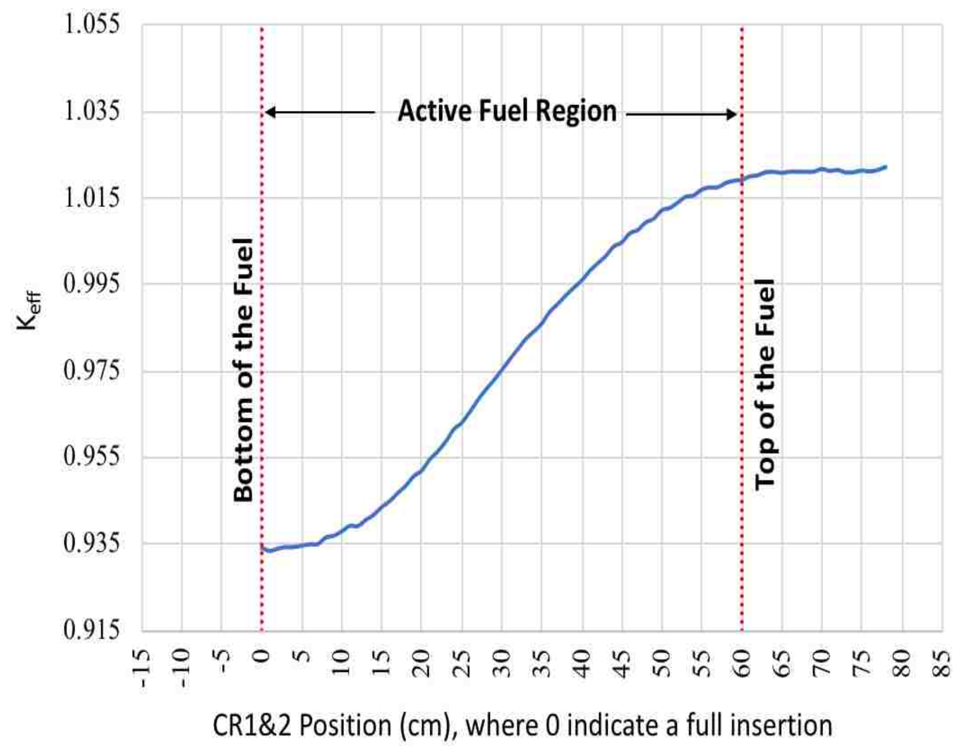

Figure 2.3. The Worth of Paired Shutdown Control Rods (CR1&2).

2.2.3. Analyzing the Optimum BeO to Graphite Thickness Ratio. Analyzing the optimum BeO to graphite thickness ratio improves the neutronic performance therefore, allow longer operation cycle for HPC core. Originally, the reflector blocks surrounding the core of HPC was only filled with graphite. An optimum thickness ratio of BeO/graphite was determined based on its effects on k_{eff} and peak-to-average flux ratio. MCNP simulation were performed starting with reflector blocks containing 100% graphite, and subsequent introduction of BeO slabs in the reflector in step of 0.5 *cm* thickness. The total thickness of the reflector was kept constant regardless of its BeO thickness. Reflector slabs were in vertical orientation with thickness variation in direction orthogonal to the core's vertical axis. In all cases with composite BeO/graphite reflectors, the reflector blocks were oriented such that the BeO side bounded the core. The k_{eff} and peak-to-average flux ratio for varying BeO/graphite composites are shown in Figure 2.4. The x-axis represents the block thickness

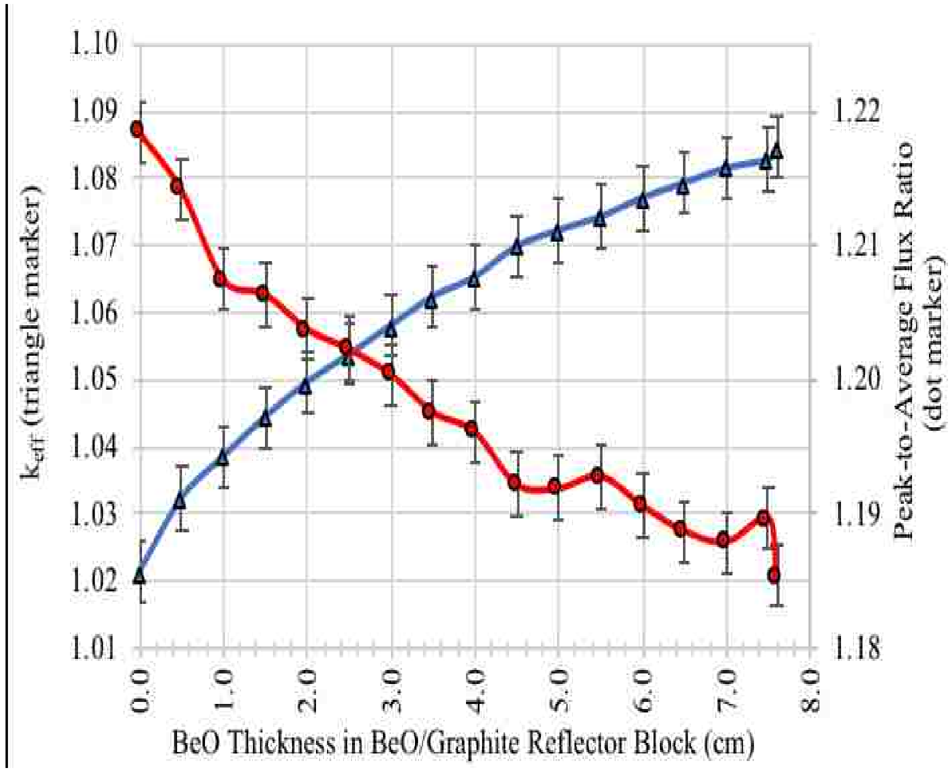

Figure 2.4. Impact of BeO/Graphite Composite Reflector Block on Multiplication Factor and Peak-to-Average Flux Ratio. 0 *cm* implies 100% graphite block while 7.6 *cm* implies 100% BeO block.

in centimeters, starting from 0.00 *cm* (side adjacent to the core center) to 7.6 *cm* (block outer region). The left y-axis represents k_{eff} (triangle markers) where the right y-axis represents the peak-to-average flux ratio (round markers).

When the whole block was graphite (at 0.00 *cm* thickness) the k_{eff} was determined to be 1.0223 and the peak-to-average flux ratio was 1.2185. When 0.5 *cm* BeO was applied, the k_{eff} increased and the peak-to-average flux ratio decreased. Having a full BeO block significantly increased the k_{eff} up to 1.08747 and decreased the peak-to-average flux ratio to 1.1854. It is desirable to minimize BeO thickness in the composite reflector block due to the high price of beryllium. MSTR current limitation on excess reactivity is 1.5% delta-k/k [36]. Since the HPC is higher in power level, 3 times the current excess reactivity limit was assumed. This implies a maximum allowable k_{eff} of 1.04712. A BeO thickness within 1.5

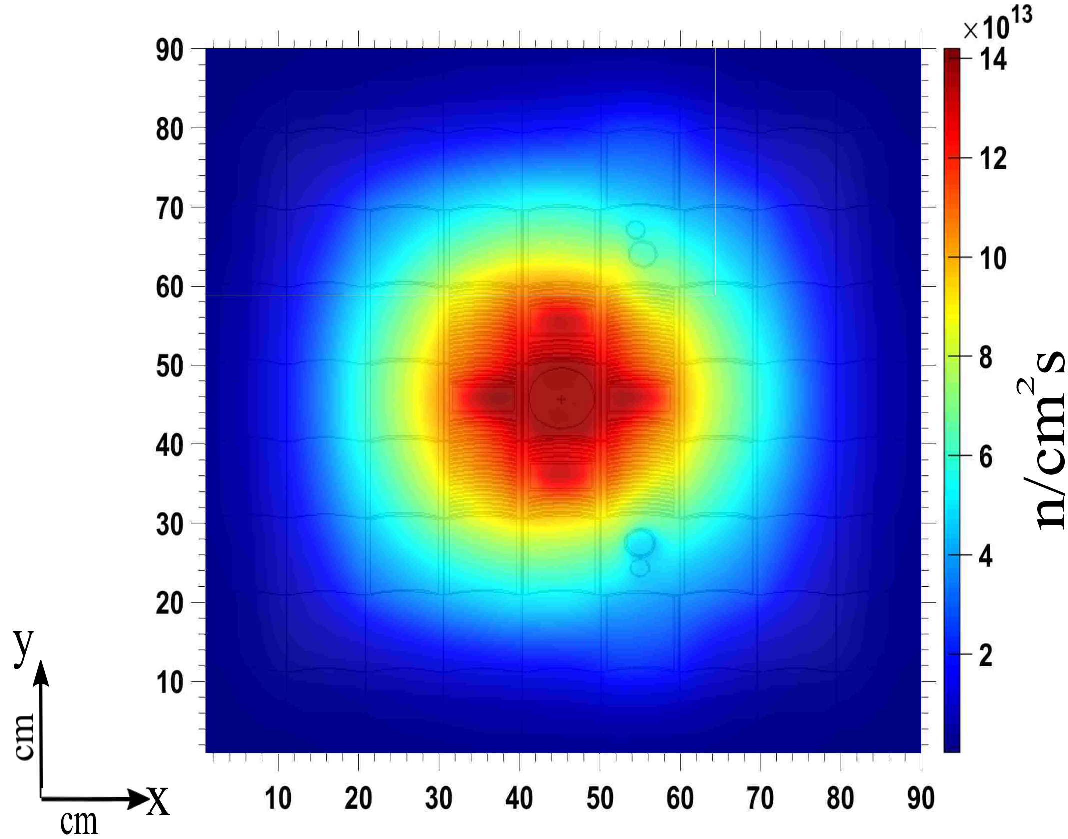

Figure 2.5. Neutron Flux Profile for HPC Core at 2 MW.

cm satisfied this limit, see Figure 2.4. The peak-to-average flux ratio (which characterize the flatness of flux profile) were statistically identical at BeO thickness of 1 *cm* and 1.5 *cm*. A BeO thickness of 1 *cm* was chosen for the reflector composite. With 1 *cm* BeO thickness, k_{eff} was 1.03853 and the peak-to-average flux ratio was 1.2075, see Figure 2.4

2.2.4. Neutron Flux Map and Capabilities. The neutron flux profile for MSTR-HPC core is shown in Figure 2.5. The central region of the reactor core has the highest neutron flux (in darkest red color) which is the FT zone. At 2 MW, the total neutron flux calculated by MCNP at the FT facility is $1.42\times10^{14} \pm 1.78\times10^{12}$ $n\ cm^{-2}\ s^{-1}$. For the BRT and CRT, the total neutron flux calculated by MCNP are $8.23\times10^{13} \pm 6.48\times10^{12}$ $n\ cm^{-2}\ s^{-1}$ and $4.15\times10^{13} \pm 4.63\times10^{12}$ $n\ cm^{-2}\ s^{-1}$ respectively.

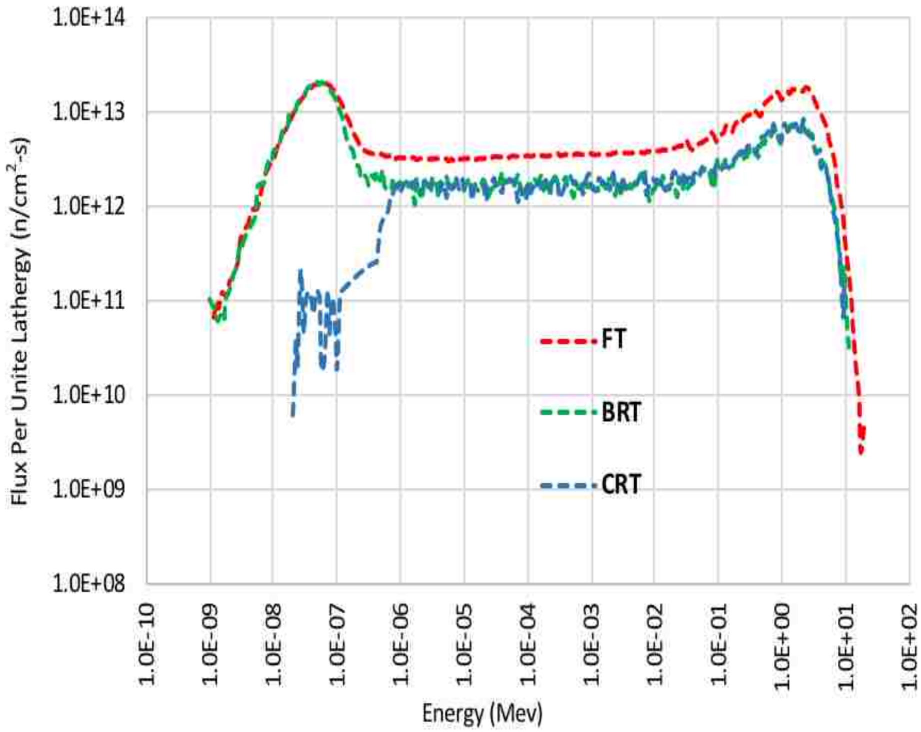

Figure 2.6. Neutron Flux Spectrum In-Core Irradiation Facilities for HPC at 2 MW.

Figure 2.6 and Table 2.3 presented the neutron flux spectrum in-core irradiation facilities for HPC. At FT facility, the fast flux was the highest contribution by 35.52% of the total produced flux, where thermal and resonance contributed 32.21% and 32.28% respectively. For BRT facility, thermal flux contributed 49.77% of the total produced flux, where resonance and fast flux contributed 26.40% and 23.84% respectively. For CRT facility, resonance flux was the highest contribution by 51.32% of the total produced flux, where fast and thermal flux contributed 47.98% and 0.70% respectively. The most suitable facility for fast flux is FT. Also, CRT can be used for fast flux and its suitable for resonance flux as well. For thermal flux, BRT is the suitable facility.

Table 2.3. Neutron Flux Spectrum In-Core Irradiation Facilities for HPC at 2 MW.

	FT		BRT		CRT	
Thermal	4.57E+13	32.21%	4.09E+13	49.77%	2.92E+11	0.70%
Resonance	4.58E+13	32.28%	2.17E+13	26.40%	2.13E+13	51.32%
Fast	5.04E+13	35.52%	1.96E+13	23.84%	1.99E+13	47.98%
Total	1.42E+14	100.00%	8.23E+13	100.00%	4.15E+13	100.00%

Table 2.4 present a comparison of total neutron flux obtained in-core irradiation facilities for both the current MSTR core configuration (as of Figure 1.3) and the proposed HPC core (as of Figure 2.2). For the current MSTR core, the MCNP simulation performed under the same conditions for HPC except the power level which adjusted to 200 KW. As a comparison result, the HPC core allow achieving high neutron flux on all irradiation facilities, see Table 2.4. As a maximum total neutron flux achieved, HPC is higher by two orders of magnitude which proves its capability for enhancing neutron flux spectrum. Keeping in mind that HPC core has only 8 fuel-bearing elements compared to the current MSTR core which has 19 fuel-bearing elements.

Table 2.4. Comparison of Total Neutron Flux In-core Irradiation Facilities for Both Configurations.

	Current MSTR Core			MSTR-HPC Core		
	In-Core Irradiation Facilities					
	HC	BRT	CRT	FT	BRT	CRT
Total Neutron Flux ($n\ cm^2\ s^{-1}$)	9.01E12 ± 6.77E11	5.26E12 ± 4.79E11	1.73 E12 ± 2.82E11	1.42 E14 ± 1.81E12	8.25E13 ± 6.62E12	4.22 E13 ± 4.77E12

2.2.5. Burnup Analysis. The burnup analysis was performed for HPC assuming the thickness of reflector blocks' materials are 1 *cm* for BeO and 6.6 *cm* for graphite. MCNP6 was used to track fuel burnup at 2 MW. The potential operation time for HPC core

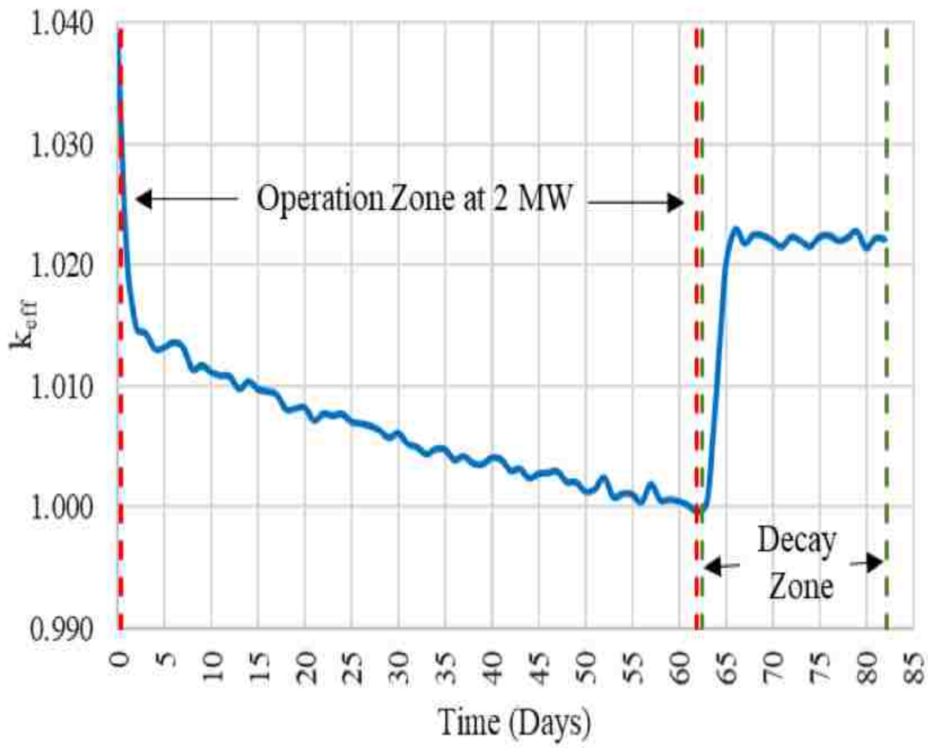

Figure 2.7. Potential Operation Time for HPC Core at 2 MW.

is presented in Figure 2.7. The reactor supported 61 days of continuous full power operation before subcriticality. At zero-time step, the calculated initial k_{eff} was 1.03853 and dropped to 0.99964 (subcritical) on day 62 of full operation. The burnup simulation included 20 days post-shutdown decay. In the first day of decaying, the calculated k_{eff} was 1.00035 and increased with time till 1.02291 which after 4 days of decaying (at 66 days, see Figure 2.7). Beyond the first 4 days of decay, the k_{eff} experienced no significant change. Due to the early plateau of k_{eff} value after shutdown, a cooling period of 10 days was assumed for the HPC core.

The post-burnup actinides inventories are summarized in Table 2.5. It should be noted that the mass for both of U-235 and U-238 didn't change by much. The mass for Pu-239 after 62 days of full operation reported to be 14.1 *g* and it increases to 15.6 *g* after

10 days of decaying. This increase is due to the decay of short-lived U-239 and Np-239 into Pu-239. The calculated total fissile materials at 0, 62 and 72 days were 6153, 6011 and 6013 *g* respectively.

2.2.6. Determination of Hot-Channel. The hot-channel was determined in both clean core (zero burnup and no poison buildup) and burned core. In HPC core, there is a total of 112 fuel plates. Figure 2.8 illustrated the sequence of fuel plates in each fuel element. For each fuel element, the fuel plates were numbered 1 to 18. In case of control rod-fuel element, plates number 6 to 13 were removed to accommodate the control rods insertion "control rod channel". Control rods channel is filled with water. Assuming clean core, the energy deposition for each fuel plates are plotted in Figure 2.9. The hottest fuel plate was determined to be fuel plate number 14 (FP#14) in control rod number 4 (CR4). CR4 is located at E4 position in HPC core, see Figure 2.2 Thu, FP#14 is adjacent to control rod channel (CR is fully withdrawn).

The calculated power distribution for FP#14 was 32.42 kW which is the highest among the other fuel plates. FP#14 contributes 1.62% of the total power distribution. It should be noted that the power distribution in FP#14 varies along the width of fuel plate and peak sharply at the edge. This is due to the increase in the local water-to-fuel ratio near to the edge of fuel meat. For clean core, the hot-channel is located between FP#14 and FP#15 of CR4.

The determination of the hot-channel for burned core was performed after incorporating the burned materials in the MCNP model and tallying energy deposition. There was no shift of the hot-channel which remained between FP#14 and FP#15 for burned core as it was for the clean core. For burned core, the hottest fuel plates remained FP#14 of CR4. The calculated power distribution for FP#14 was 32.31 kW which has 1.61% as contribution of the total power distribution. For both clean core and burned core, it should be noted that most of the fuel plates adjacent to the control rod channel "water" are having non-uniform significant burnup compared to average fuel plates. With more time of operation, higher burnup in these specific fuel plates will affect the reactivity of the core. Therefore, rotating the control rods-fuel elements by 90 degree should be evaluated in future study.

Table 2.5. HPCs' Significant Radionuclide Inventories.

Isotopes	Mass (g)		
	0 Days	62 Days	72 Days
U-235	6.15E+03	6.00E+03	6.00E+03
U-236	0.00E+00	2.79E+01	2.93E+01
U-238	2.53E+04	2.53E+04	2.53E+04
U-239	0.00E+00	6.03E-03	-
Np-237	0.00E+00	1.12E-01	1.36E-01
Np-239	0.00E+00	8.54E-01	1.10E-01
Pu-238	0.00E+00	6.23E-04	7.92E-04
Pu-239	0.00E+00	1.41E+01	1.56E+01
Sr-90	0.00E+00	2.84E+00	2.97E+00
Tc-99	0.00E+00	3.13E+00	3.49E+00
Xe-135	0.00E+00	2.26E-02	-
Cs-137	0.00E+00	4.65E+00	4.88E+00
Sm-149	0.00E+00	3.06E-01	3.52E-01

2.3. CFD MODELING FOR HOT-CHANNEL

Previous studies of the HPC core involved neutronic evaluations including criticality calculation, determination of neutron flux profile and spectrum, safety shutdown margin, determination of hot-channel (clean core and burned core) and burnup analysis [2, 3]. Further study is needed especially in terms of thermal hydraulic behavior. Thermal hydraulic

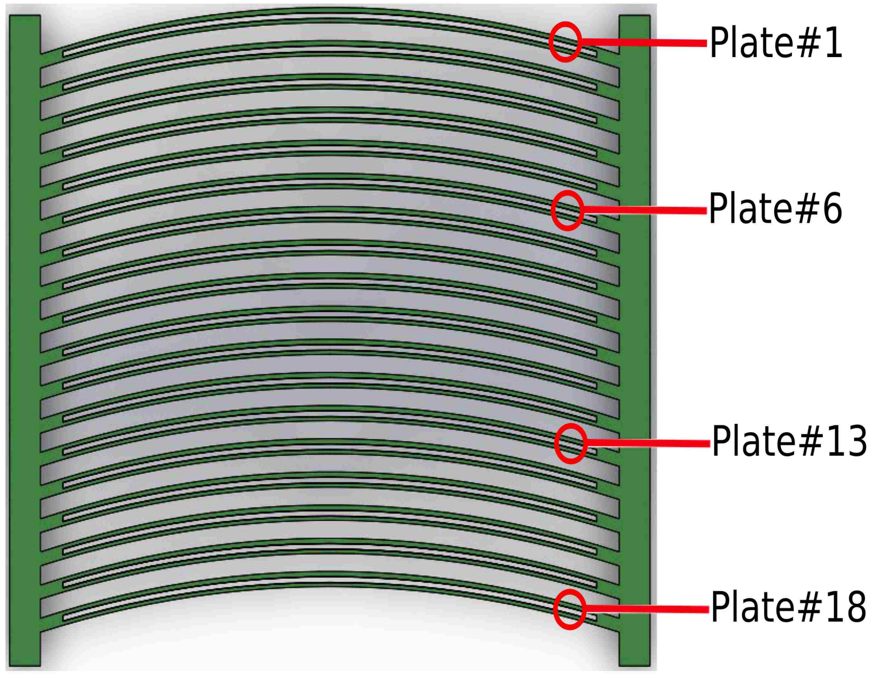

Figure 2.8. Sequence of Fuel Plates in Each Fuel Elements.

analyses focused in heat removal and cooling requirements. Heat is primarily released in the structural materials of fuel plates and transferred from fuel to the adjacent coolant “water” channel. If the heat is not transfer and removed properly, the structural materials’ temperature will increase until it exceeds the temperature limit. This will cause melting and releasing radioactive materials. The maximum heats over the entire core is generated in the hottest fuel plate. Under normal operation conditions, the reactor can be considered to operate safely if the generated heat in hottest fuel plates can be safely transferred through the structural materials and safely removed by the coolant-channel. This section will investigate the modeling of the HPCs’ hot-channel using ANSYS Fluent. The goal herein is to study the thermal-hydraulic of HPCs’ hot-channel from safety limits perspective. This can be achieved by investigating heat transfer and coolant temperature for 3D model representing

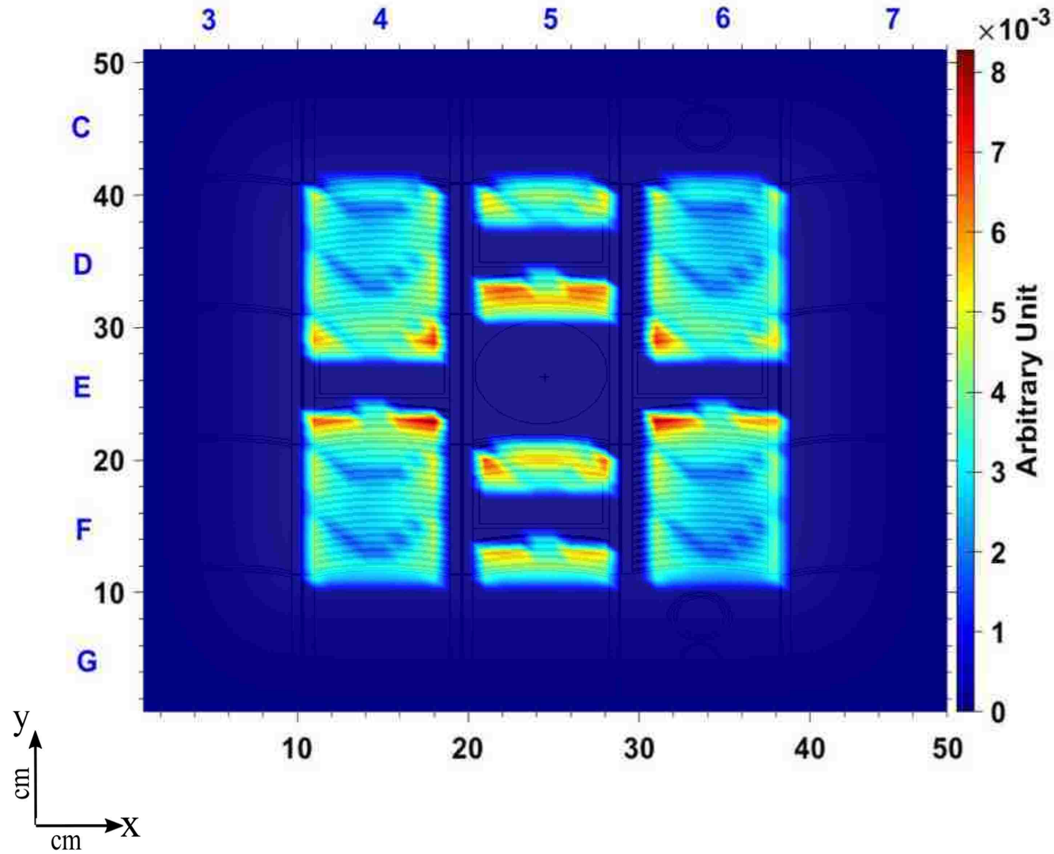

Figure 2.9. Hottest Fuel Plates for HPC Clean Core (C-G and 3-7 grid reference labels; blue colored).

HPCs' hottest fuel plates and hot-channel. Safety limit included U-10Mo melting point (1150 ^{0}C), the clad melting points (660 ^{0}C) and delamination limits of U-10Mo plate-type fuel (~ 550 ^{0}C) [37, 38]. Also, the water boiling point at 178.8 KPa which is ~ 391 K [39].

2.3.1. Model Specification and Conditions. The model contains two parallel curved half-fuel plate with a single coolant-channel in between. Figure 2.10 represent the cross-sectional view of the model. Same geometries for HPCs' curved fuel plate and the coolant-channel was applied. The two curved fuel plates were halved to allow concentrating the released heat to the direction of coolant-channel. The model was designed and set up using ANSYS Fluent [27]. The computational domain of the model was 62.5 *cm* tall, 1.25 *cm* width and 6.68 *cm* length. The calculated Reynold number for coolant-channel

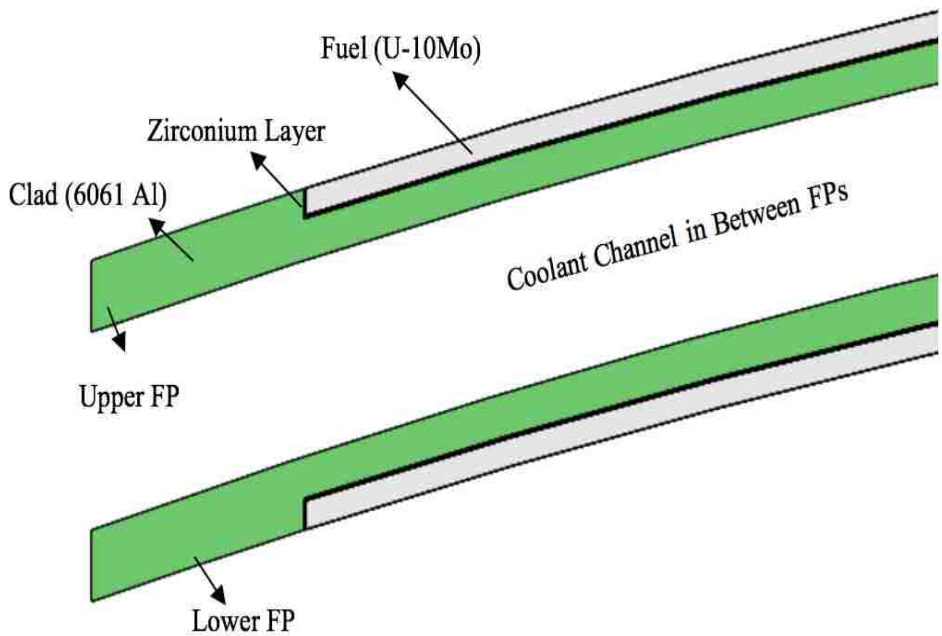

Figure 2.10. Cross-Sectional-View of the Simulated Model.

was 3799. Thus, simulation was performed assuming a steady-state single-phase turbulent flow. Forced circulation was assumed for removing heat with inlet temperature of 322.15 K for coolant-channel. For conservative analysis the total power produced (32.42 KW) was divided between the two fuel plates. Each fuel plate produced 16.21 KW. The calculated total volumetric heat rate was 1744.5 W/cm^3. The heat generation was defined as uniform volumetric heat for each fuel region.

Thermal hydraulic parameters for the model are presented in Table 2.6. Based on the design, ΔT was 12 K and the total coolant cross-sectional area for the active core was calculated to be 332.5 cm^2. The calculated total mass flow rate was 39.86 kg/s. For coolant-channel, the calculated cross-sectional area and mass flow rate were 2.071 cm^2 and 0.248 kg/s respectively. The determined inlet velocity for the core was 1.213 m/s. Considering 26 ft deep-water as of MSTR reactor pool, the calculated outlet pressure was 178.8 KPa. The surface walls bounded the coolant-channel and the two fuel plates were assumed to be

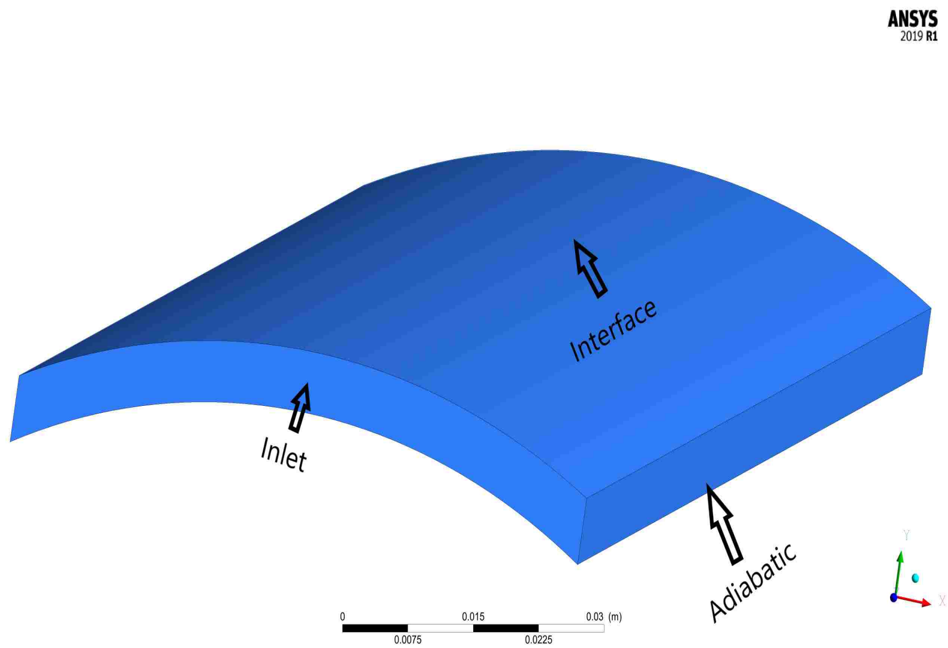

Figure 2.11. Boundary Conditions of Coolant-Channel.

adiabatic, see Figure 2.11. No-slip condition was applied for the interface of coolant-channel with convex and concave sides of fuel plate. This implies zero velocity at the interfacing surfaces (clad with coolant) which will result in high temperature than a real-life situation. Thus, for conservative analysis the no-slip condition was applied. No nucleate boiling is allowed throughout the simulated model. The model boundary conditions and solving algorithm are presented in Table 2.7. The inlet and outlet condition of the computational domain were set to be mass flow rate and pressure respectively. Standard K-W model (SST) was chosen for solving Reynold-averaged Navier-Stokes equations. The governing equation for conservation of mass, momentum and energy were solved by FLUENT [27].

For better evaluation of heat transfer over small region, the thin zirconium layer surrounds the fuel meat was defined as thermal contact conductance (TCC) [27]. TCC was determined by dividing the thermal conductivity of zirconium by its thickness; TCC = 90.55 W/cm^2 k. Three locations were assigned for data extraction of the simulated coolant model namely, inlet, middle and outlet.

Element sizing function was applied to mesh the fuel plates. Due to the limitation of computational resource, the smallest element size that can be successfully generated was 1 mm. Edge sizing function was applied along the height, length and width of coolant-channel. Several grid numbers were considered for evaluating mesh sensitivity, see Figure 2.12. The considered total nodes were 24689, 35497, 40749, 65488, 91216, 107397, 268362, 351251, 451005, 501483, 679937, 758315 and 836693. From the smallest considered grid number to the maximum, the temperature variation for coolant-channel and fuel-center-line were 2.97 and 4.70 K respectively. Grid number with total nodes of 679937 (see Table 2.8) was considered for performing the simulation. Such selection help minimizing the computational requirements. Figure 2.13 represents the generated mesh for all region of the model.

2.3.2. Result and Discussion. 232 CFD iteration was found to be sufficient for stabilizing the outlet temperature of coolant-channel. The determined average temperature for coolant-channel at the outlet of the model was 341.12 K. Thus, the calculated ΔT was 18.89 K. The temperature distribution profile along the height of coolant-channel is shown in Figure 2.14. The temperature at the inlet region (red-line) was flat at the center 322.15 K along with a little increase at the interfacing regions with convex and concave sides of fuel plate. No significant heat generated at the inlet region and the flow is not fully developed yet. At the middle of coolant-channel (blue-line), temperature at both interfacing regions reached a maximum of 383 K. However, at the center of the middle region of coolant, the temperature reached 333 K. For both coolant interfaces (convex and concave sides of fuel plate), the temperature distribution was similar due to the similarity of simulation

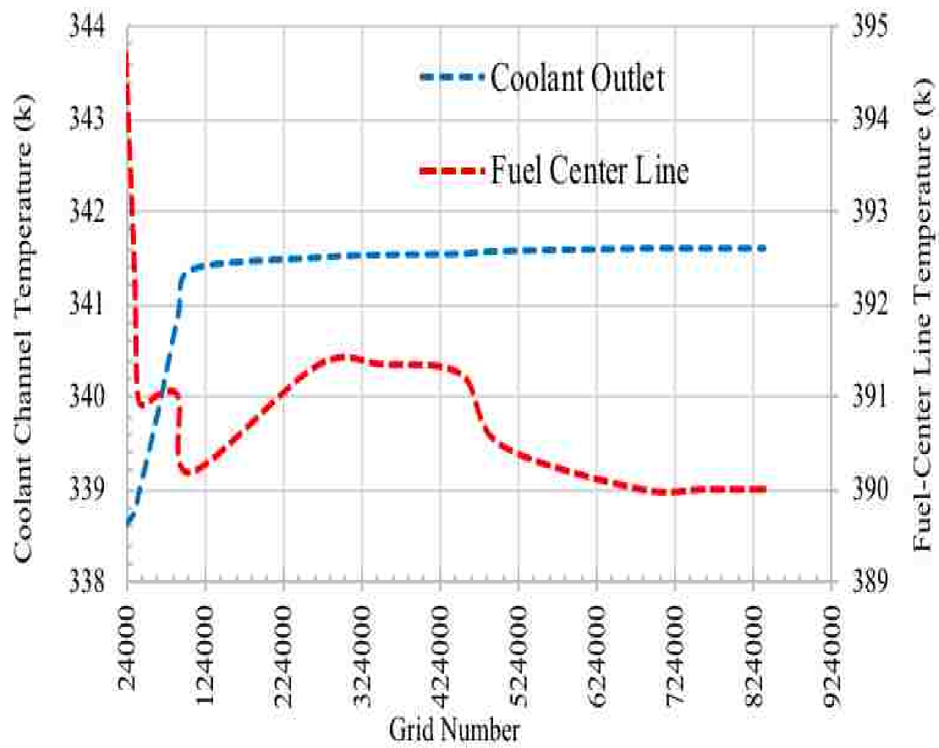

Figure 2.12. Evaluation of Mesh Sensitivity.

conditions. At the outlet of coolant-channel (green-line), temperature at both interfaces reached 359 K. For the center region, the flow exited the model at a temperature of 341 K, see Figure 2.14. The reasons for lower temperatures at the interfacing regions for the coolant outlet are due to 1) no slip interface condition between the plate and the coolant and, 2) the fuel which is the heat source does not extend to the inlet and the outlet edges of the fuel plate. Hence, the coolant at the top and of the interface receives no direct heat from the fuel meat. In addition, the top of cladding in both fuel plate was set to be adiabatic for conservative analysis. It worth noticing that in the monitored locations of coolant-channel, the temperature didn't reach the boiling point of water at the considered pressure. Boiling point of water at 178.8 KPa reported to be ~ 391 K [39].

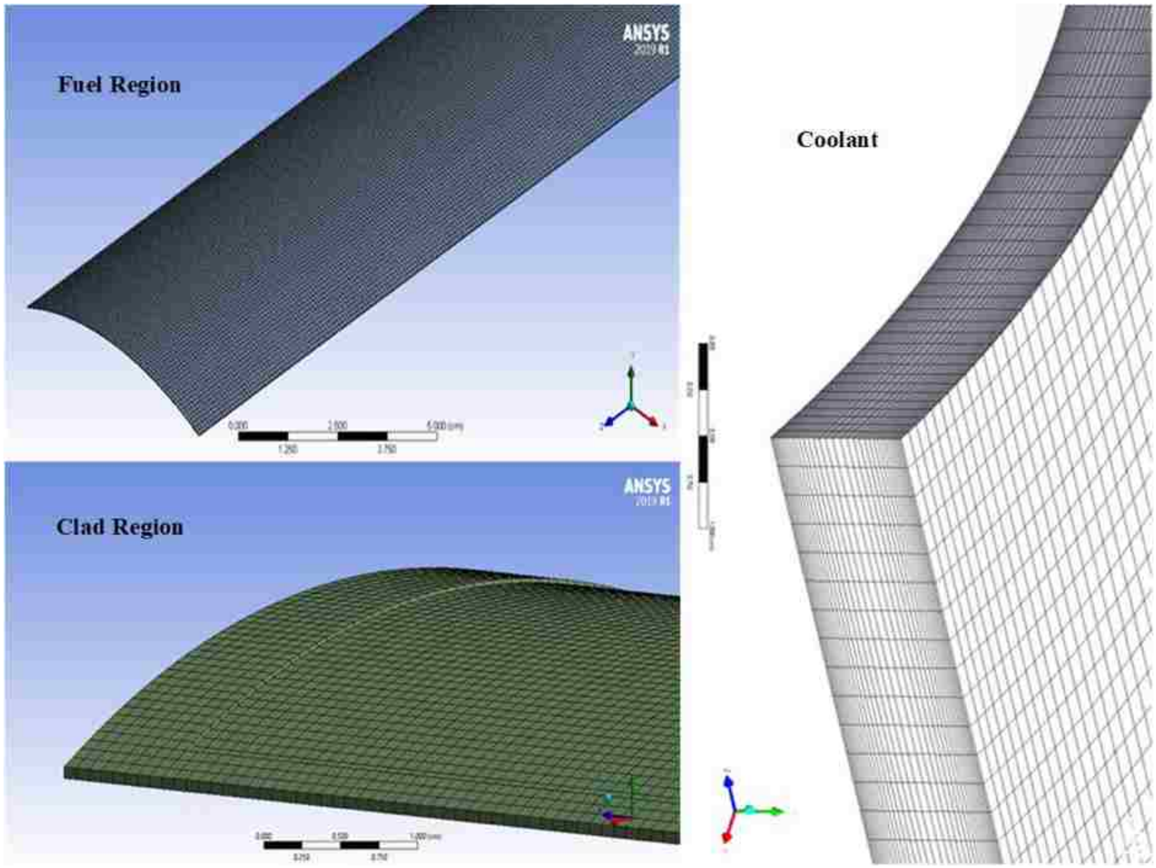

Figure 2.13. Generated Mesh for all Regions of the Model.

The temperature contours for convex sides of fuel plate (containing fuel and clad regions) is shown in Figure 2.15 and Figure 2.16, respectively. The temperature contours for concave sides of fuel plate (containing fuel and clad regions) are shown in Figure 2.17 and Figure 2.18, respectively. The maximum temperature attained in the convex and concave sides of fuel regions were 391.76 and 390.37 K, respectively. The maximum temperature attained in the convex and concave sides of aluminum-clad regions were 389.92 and 388.54 K, respectively.By considering the heat generated in the hottest fuel plate of HPC core, the determined temperature for fuel plate regions were below the safety limits. Safety limit included U-10Mo melting point (1150 ^{0}C), the clad melting points (660 ^{0}C) and the delamination limits of U-10Mo plate-type fuel (~ 550 ^{0}C) [37, 38]. The pressure and

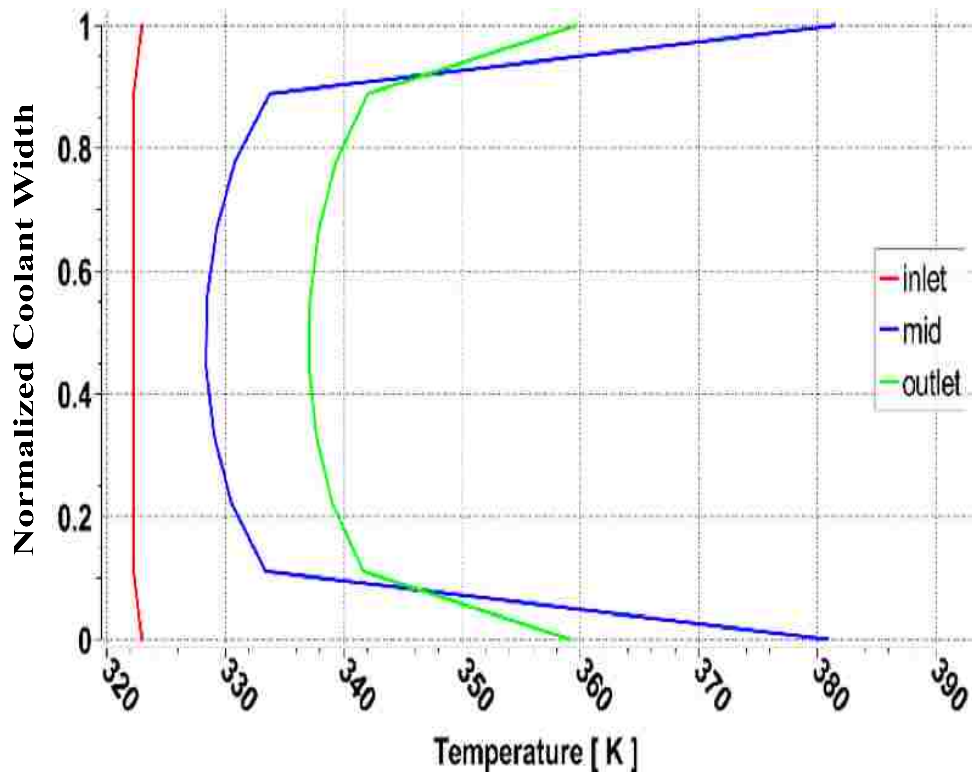

Figure 2.14. Temperature Distribution of Coolant-Channel.

velocity profiles are shown in Figure 2.19 and Figure 2.20, respectively. At coolant inlet, velocity started at 0.664 cm/s and increased towards 0.8 cm/s at the outlet of the coolant-channel. The presented pressure profile is gauge pressure. The determined pressure difference (outlet to inlet) was 520 Pa. At full operation power of HPC core, the mass flow rate of 39.86 kg/s (10.644 gallon/s) was sufficient for removing the generated heat. An average pumping system in current market can produce such requirement. However, a pumping system with higher capability can add an extra safety assurance for removing the generated heat in HPC core.

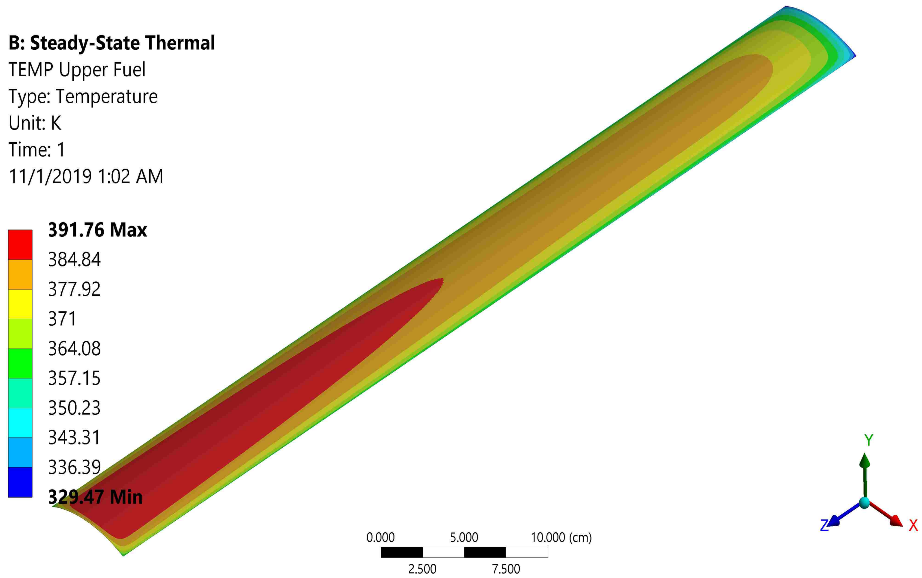

Figure 2.15. Temperature Contours for Convex Side of Fuel Region.

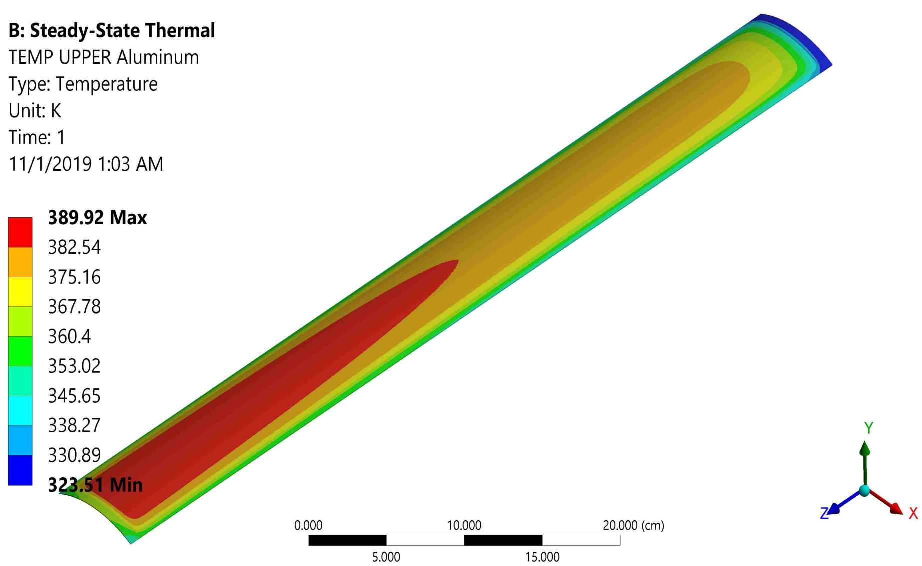

Figure 2.16. Temperature Contours for Convex Side of Clad Region.

Table 2.6. Thermal-Hydraulic Parameters.

Parameter	Condition
Fuel	U-10Mo
Fuel Thermal Conductivity (W/cm k)	0.176
Fuel Density (g/cm^3)	16.09
Coolant	Light Water
Coolant Flow Direction	Upward
Water Specific Heat (J/kg k)	4181.5
Cladding	Al 6061
Cladding Thermal Conductivity (W/cm k)	1.67
Cladding Density (g/cm^3)	2.7
Zirconium Density (g/cm^3)	6.506
Zirconium Thermal Conductivity (W/cm k)	0.23
Inlet Temperature (K)	322.15
Outlet Pressure (Pa)	178788.12
Mass Flow Rate (kg/s) for Coolant	0.24823
Cross-Sectional Area for Coolant (cm^2)	2.0708
Total Power Distribution by Fuel Plates (W)	32416.06
Total Volumetric Heat Rate (W/cm^3)	1744.5
Reynold number for Coolant	3799.88
Prandtl number	4.39

Table 2.7. Boundary Conditions and Solving Algorithm.

Parameter	Condition
Turbulence Model	Standard K-W (SST)
Inlet Condition	Mass flow rate
Outlet Condition	Presser Outlet
Wall Between Fuel and Cladding	Coupled
Wall Between Cladding and Coolant	Fluid Solid Interface

Table 2.8. Mesh Characteristics.

Parameters	Value
Node of Single Fuel Region	78208
Node of Single Clad Region	89130
Total Node of Solid	334676
Total Node of Fluid	345261

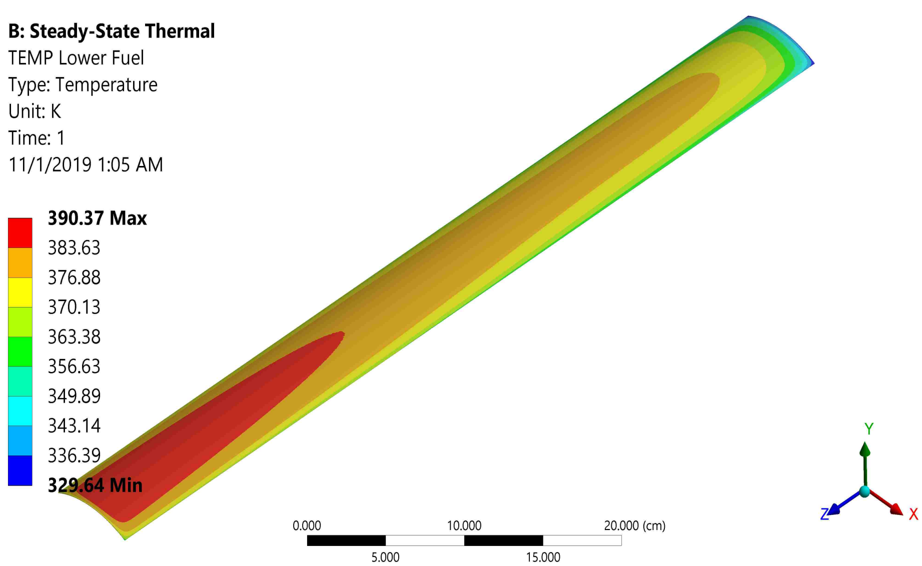

Figure 2.17. Temperature Contours for Concave Side of Fuel Region.

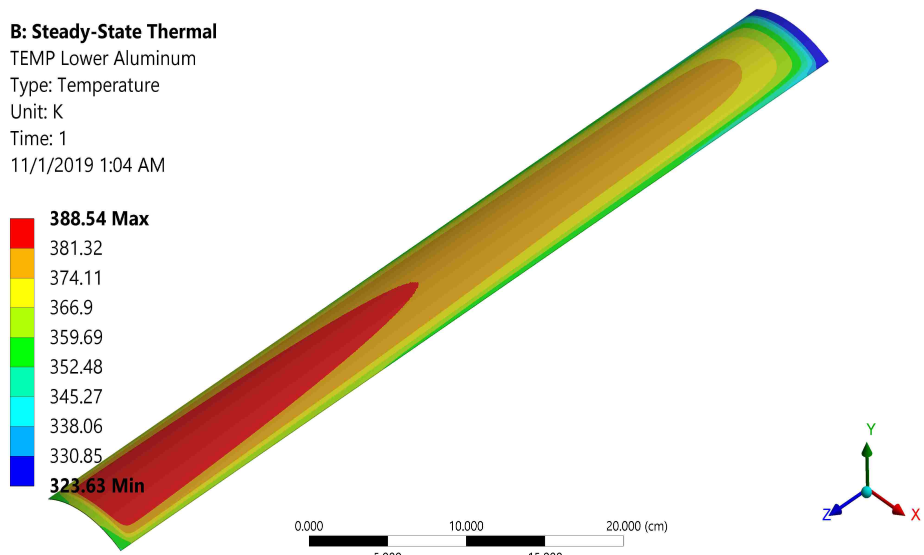

Figure 2.18. Temperature Contours for Concave Side of Clad Region.

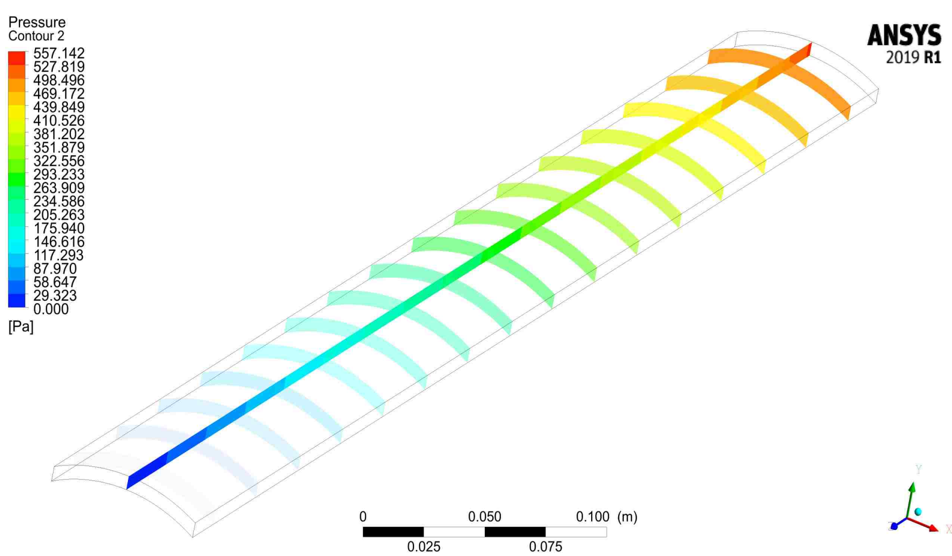

Figure 2.19. Pressure Profile of Coolant-Channel.

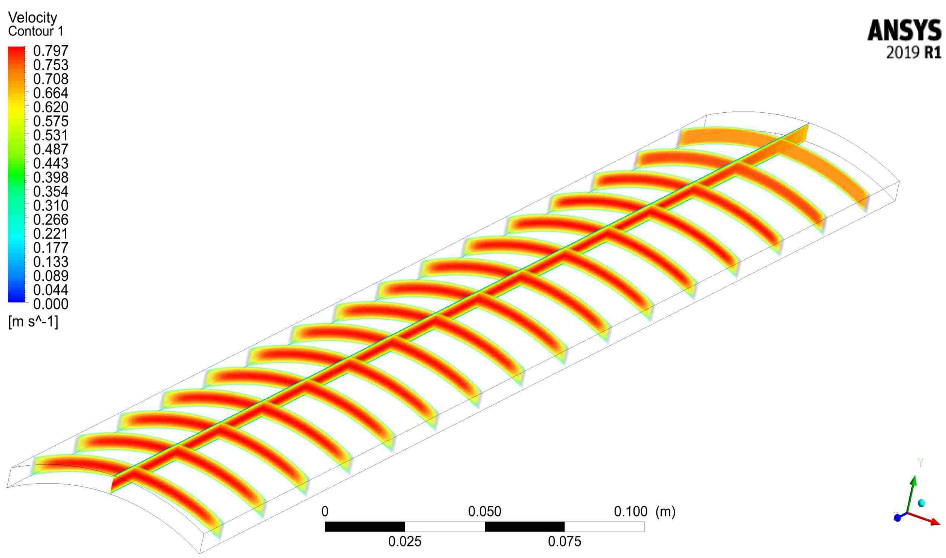

Figure 2.20. Velocity Profile of Coolant-Channel.

3. THE PROPOSED LOW-POWER CONFIGURATION (LPC)

The goal of low-power core configuration (LPC) is to enhance the reactor by the inclusion of additional irradiation facilities for core robustness in supporting multiple tests at a time. LPC considered the operation at 200 KW. The initial considered core configuration for LPC is like the HPC core configuration but with additional three in-core irradiation facilities. Fuel and control rods were the same in design as the HPC. Initial-LPC configuration is presented in Figure 3.1. The core is compact core where graphite reflector blocks surrounds the core from all sides. By performing criticality calculation using MCNP for Initial-LPC core configuration, k_{eff} was determined to be low. The determined k_{eff} was 1.00823 with an estimated standard deviation of 0.00034. This implies that a reasonable time of operation may not be maintained. In order to improve the low k_{eff}, two option were evaluated: 1) adding extra fuel to the core or 2) adopting a composite reflector blocks containing BeO and graphite as the one used for HPC. LPC configuration is this section considered the extra fuel option. The second option was investigated under flexible-power configuration (FPC) section.

The U-10Mo fuel of the HPC was the basis for the LPC. Six in-core irradiation facilities were included in the LPC core three of which are FT, BRT and CRT. The additional in-core irradiation facilities are three graphite-block irradiation facilities. The fuel element shell containing the FT facility was filled with graphite and labeled as FT-GB. Same for the BRT and CRT, the fuel elements shell contains these facilities were filled with graphite and labeled as BRT-GB and CRT-GB. Four fuel elements were added to the LPC core in order to increase the k_{eff} value. Therefore, the LPC core consists of eight fuel elements, four control rod elements and six in-core irradiation facilities (FT, BRT, CRT, FT-GB, BRT-GB, CRT-GB), see Figure 3.2. A graphite reflector blocks is included in the left side of the

	1	2	3	4	5	6	7	8	9
A									
B						GB			
C			GB	GB	GB	BRT	GB		
D		GB	BRT -GB	FE	CR1	FE	GB		
E		GB	HC	CR4	FT	CR3	GB		
F		GB	CRT -GB	FE	CR2	FE	GB		
G			GB	GB	GB	CRT	GB		
H						GB			
L									

GB: Graphite Block FE: Fuel Element CR#: Control Rod
BRT: Bare Rabbit Tube CRT: Cadmium Rabbit Tube FT: Flux Trap
BRT-GB: BRT Inside GB CRT-GB: CRT Inside GB HC: Hot Cell

Figure 3.1. Initial LPC Core Configuration.

core in order to reflect neutrons back to the core. This will allow neutron enhancement in the left side of the core which contain the new irradiation facilities (FT-GB, BRT-GB and CRT-GB).

The control rods designs remain unchanged, same as the one included in HPC core. The only changes in the control rods are the concentration of natural boron in stainless steel. The effect of increasing the concentration of natural boron on k_{eff} is presented in Figure 3.3 for LPC core. With full insertion of CR1 and 2 (pair of shutdown control rods) and with 2% of boron concentration, the determined k_{eff} for LPC core was 0.98334 with an estimated standard deviation of 0.00034, see Figure 3.3. Such value of k_{eff} is relatively close to the criticality of the core. Therefore, using control rods with 2% of boron concentration is not a good option in term of the effective safety shutdown margin for LPC. Thus, Boron concentration in control rod system for LPC core was increased to 12.6% to allow for an effective safety shutdown, see Figure 3.3.

	1	2	3	4	5	6	7	8	9
A									
B									
C			GB	GB	FE	FE	BRT		
D			GB	BRT -GB	FE	CR1	FE		
E			GB	FT- GB	CR4	FT	CR3		
F			GB	CRT -GB	FE	CR2	FE		
G			GB	GB	FE	FE	CRT		
H									
L									

GB: Graphite Block FE: Fuel Element CR#: Control Rod
BRT: Bare Rabbit Tube CRT: Cadmium Rabbit. FT: Flux Trap
BRT-GB: BRT Inside GB FT-GB: FT Inside GB CRT-GB: CRT Inside GB

Figure 3.2. LPC Core Configuration.

3.1. MCNP MODEL AND SIMULATION CONDITIONS

The LPC model was set up and modified from the previous HPCs' model using MCNP6. The involved modifications on the model were: including the three additional in-core irradiation facilities (FT-GB, BRT-GB and CRT-GB), adding four fuel elements and reconfiguring the LPC core components as of Figure 3.2. The neutronic simulation was performed, which involve criticality calculation, determination of neutron flux profile over core and flux spectrum in-core irradiation facilities, determination of control rod worth and hot-channel for clean core. k_{eff} was evaluated at room temperature with all control rod fully withdrawn. A KCODE criticality calculation was performed with 20,000 particles per cycle for a total of 300 cycles. Mesh card was set up and used along with Tally F4:N for the determination of flux profile and spectrum at 200 KW. A mesh was set up over each

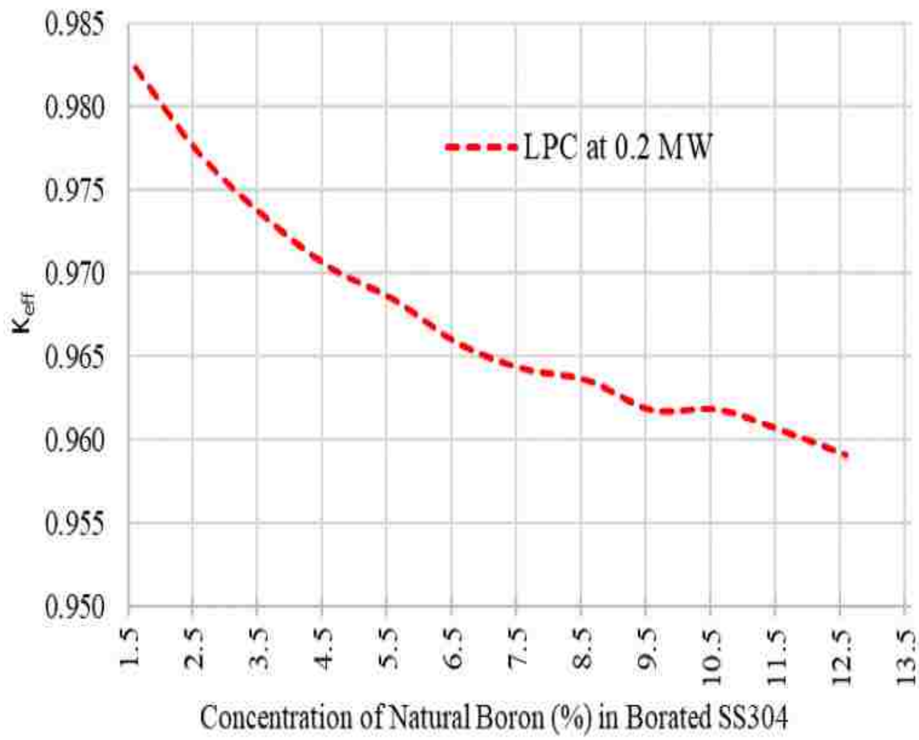

Figure 3.3. The Effect of Boron Concentration on k_{eff} for LPC Core Configuration.

fuel plate to track fission energy deposition. Also, Tally F7:N was used for tracking fission energy deposition. For the cross-section library, ENDF/B-VI was used for all isotopes in the model.

3.2. RESULTS AND DISCUSSION

This section included an evaluation of neutron multiplication factor and safety shutdown margin, calculation of flux map and spectrum, and determination of hot-channel.

3.2.1. Neutron Multiplication Factor and Safety Shutdown Margin. The determination of k_{eff} performed at room temperature with control rods fully withdrawn. The determined k_{eff} is 1.05568 with an estimated standard deviation of 0.00037. A several assumption has been applied for the safety shutdown margin; 1) a pair of two control rods

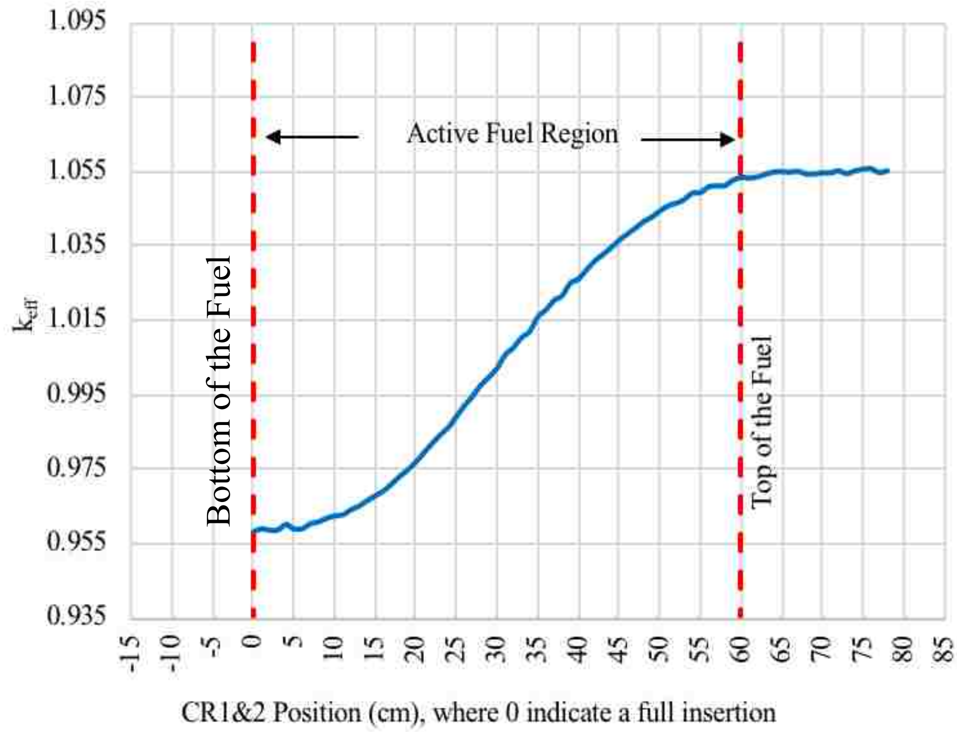

Figure 3.4. The Worth of Paired Shutdown Control Rods (CR1&2).

are the shutdown control rods, 2) the third control rod is the extra shutdown control rod and 3) the fourth control rod is the regulating control rod. All the control rods positions (see Figure 3.2) have been tested for the determination of optimum positions for the pair shutdown control rods, extra shutdown control rod and the regulating control rod. Full insertion of CR1 and CR2 was determined to be the most effective pair of control rod for shutdown. By the full insertion of CR1 and 2, k_{eff} was 0.95910 with an estimated standard deviation of 0.00036. CR4 and CR3 were assigned to be the extra shutdown control rods and the regulating rod, respectively. The control rod worth for CR1 and CR2 (pair of shutdown control rods) are plotted in Figure 3.4.

3.2.2. Neutron Flux Profile and Capabilities. Figure 3.5 presented the neutron flux profile of the LPC core at 200 KW. The picture of the actual core of LPC is transparent over neutron flux profile for a better visualization. Figure 3.5 showed a horizontal line of

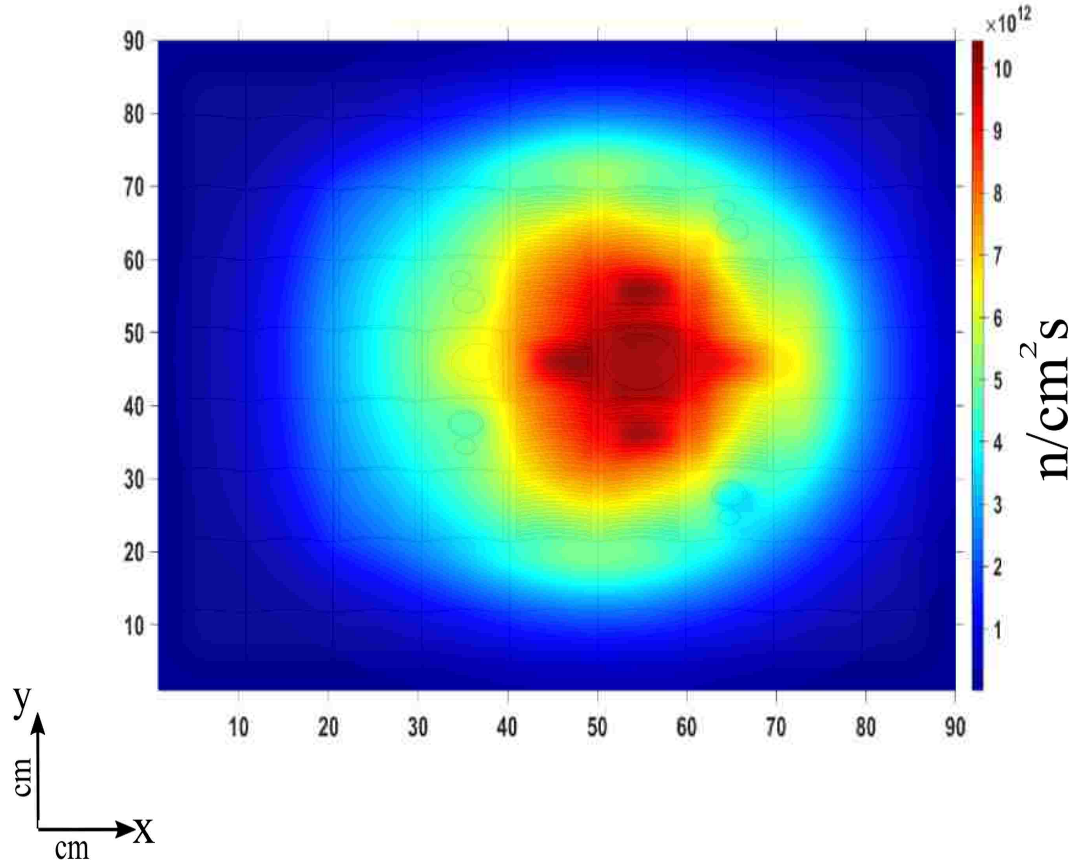

Figure 3.5. Neutron Flux Profile for LPC Core Configuration at 200 KW.

symmetry. This provides flexibility in positioning irradiation facilities either on the upper or lower sides of the core, considering XY-view. As can be seen in Figure 3.5, the highest neutron flux region (in darkest red color) is the middle region of the core which is the FT region. At the FT region, the total neutron flux calculated by MCNP at 200 KW is $1.03\times10^{13} \pm 1.52\times10^{11}$ $n\ cm^2\ s^{-1}$. For the BRT and CRT, the total neutron flux calculated by MCNP are $6.42\times10^{12} \pm 5.72\times10^{11}$ and $3.28\times10^{12} \pm 4.07\times10^{11}$ $n\ cm^2\ s^{-1}$, respectively. For graphite-block irradiation facilities (FT-GB, BRT-GB and CRT-GB) the total neutron flux calculated by MCNP are $6.54\times10^{12} \pm 1.53\times10^{11}$, $7.02\times10^{12} \pm 6.45\times10^{11}$ and 4.93×10^{12} $\pm$ 4.94×10^{11} $n\ cm^2\ s^{-1}$, respectively.

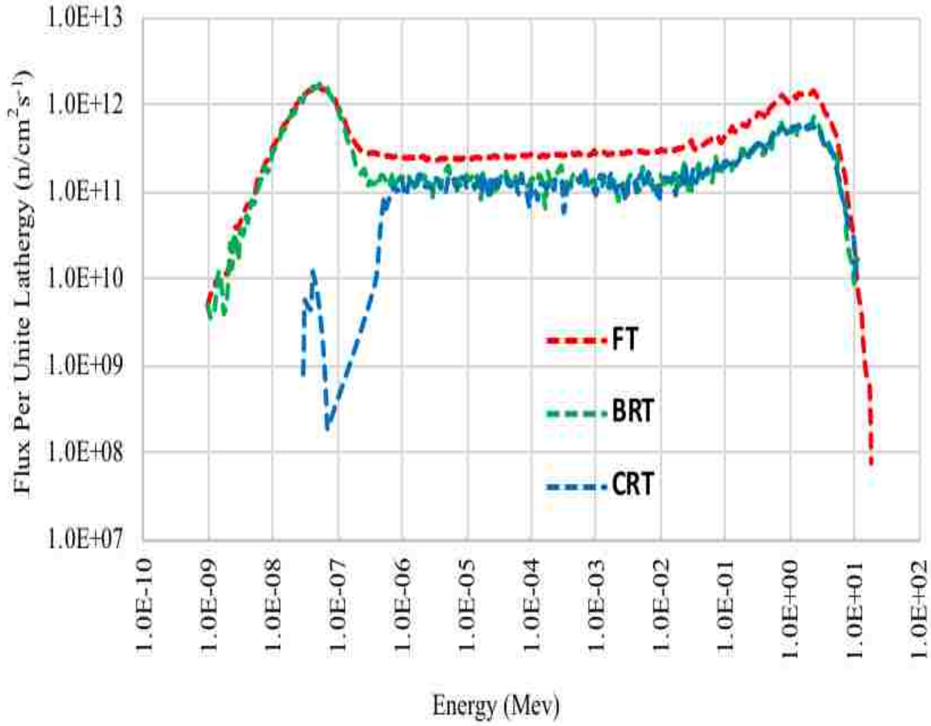

Figure 3.6. Neutron Flux Spectrum In-Core Irradiation Facilities-A for LPC at 200 KW.

Figure 3.6 and Figure 3.7 are representing the neutron flux spectrum for LPCs' in-core irradiation facilities. Table 3.1 contains the contribution percentages of thermal, epithermal "resonance" and fast flux in each irradiation facilities. For fast neutron flux, FT is the most suitable facility. This is due to the 35.82% of the total produced flux in FT facility was fast flux which was calculated to be $3.69 \times 10^{12} \pm 4.29 \times 10^{10}$ $n\ cm^{-2}\ s^{-1}$. CRT-GB, BRT-GB and FT-GB facilities can be you used for fast flux as well, see Table 3.1 and Figure 3.7. BRT is the most suitable facility for thermal neutron flux. This is because 48.23% of the total produced flux in BRT facility was thermal flux which was calculated to be $3.10 \times 10^{12} \pm 1.69 \times 10^{11}$ $n\ cm^{-2}\ s^{-1}$. For resonance and thermal flux, FT facility can be used. All the graphite-block irradiation facilities can be used for resonance flux, see Table 3.1 and Figure 3.7.

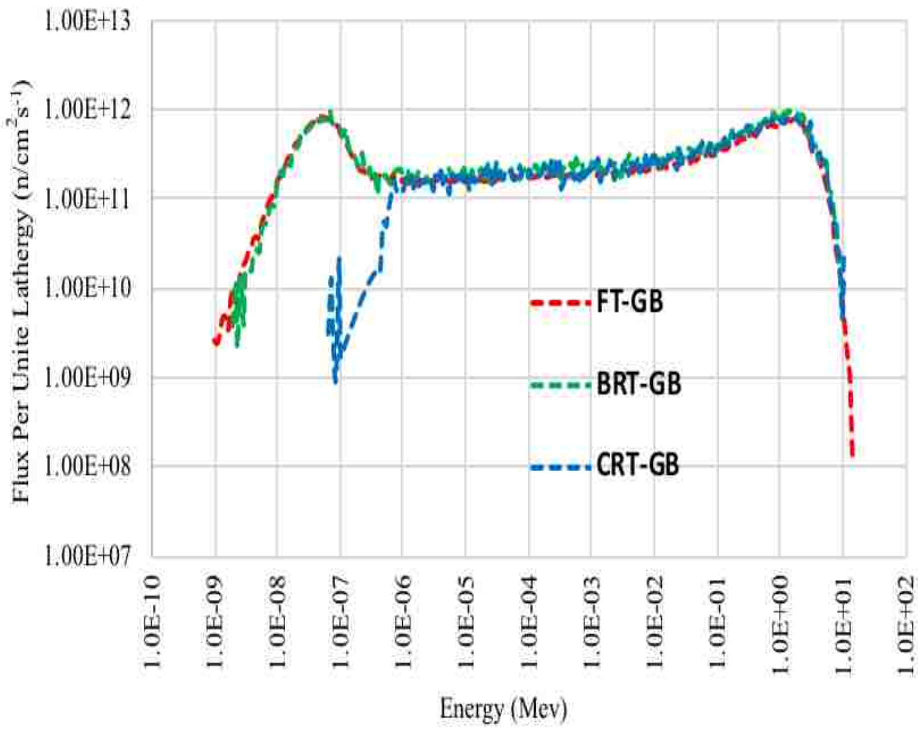

Figure 3.7. Neutron Flux Spectrum In-Core Irradiation Facilities-B for LPC at 200 KW.

3.2.3. Hot-Channel Determination. For high-power core, the hot-channel determination is important to point out the spot of maximum generated heat and burnup. In low-power core hot-channel determination allow for better understanding of the reactivity of the core along with the burnup. For LPC, hot-channel was determined for the clean core (fresh fuel with zero burnup and no poison buildup). The MCNP6 was used for hot-channel determined. Mesh card was set up for each fuel plates and fission energy deposition was tracked. There is a total of 184 fuel plates in LPC core. For LPC clean core, the fission energy deposition is plotted in Figure 3.8. The hottest fuel plate over the entire core was in control rods number 4 (CR4 occupied position E5, see Figure 3.2). Fuel plate number 14 (FP#14) was the hottest fuel plate which is the adjacent fuel plate to the control rod channel “water”. Therefore, the hot-channel is located between FP#14 and FP#15 of CR4. The calculated power contribution for FP#14 was 2.3 KW, representing 1.115% of the total

Table 3.1. Neutron Flux Spectrum In-Core Irradiation Facilities for LPC.

	FT		BRT		CRT	
Thermal	3.30E+12	32.01%	3.10E+12	48.23%	1.58E+10	0.48%
Resonance	3.31E+12	32.17%	1.68E+12	26.19%	1.60E+12	48.84%
Fast	3.69E+12	35.82%	1.64E+12	25.58%	1.66E+12	50.68%
Total	1.03E+13	100.00%	6.42E+12	100.00%	3.28E+12	100.00%
	FT-GB		BRT-GB		CRT-GB	
Thermal	1.86E+12	28.39%	1.73E+12	24.58%	1.72E+10	0.35%.
Resonance	2.44E+12	37.26%	2.77E+12	39.37%	2.51E+12	50.94%
Fast	2.25E+12	34.35%	2.53E+12	36.06%	2.40E+12	48.71%
Total	6.54E+12	100.00%	7.02E+12	100.00%	4.93E+12	100.00%

power distribution. As can be seen, there is a variation of power distribution among the width and the length of FP14 similar to the hot-channel of HPC core. The power peak sharply at the edge of FP#14 which is due to the increase of local water-to-fuel ratio in these regions.

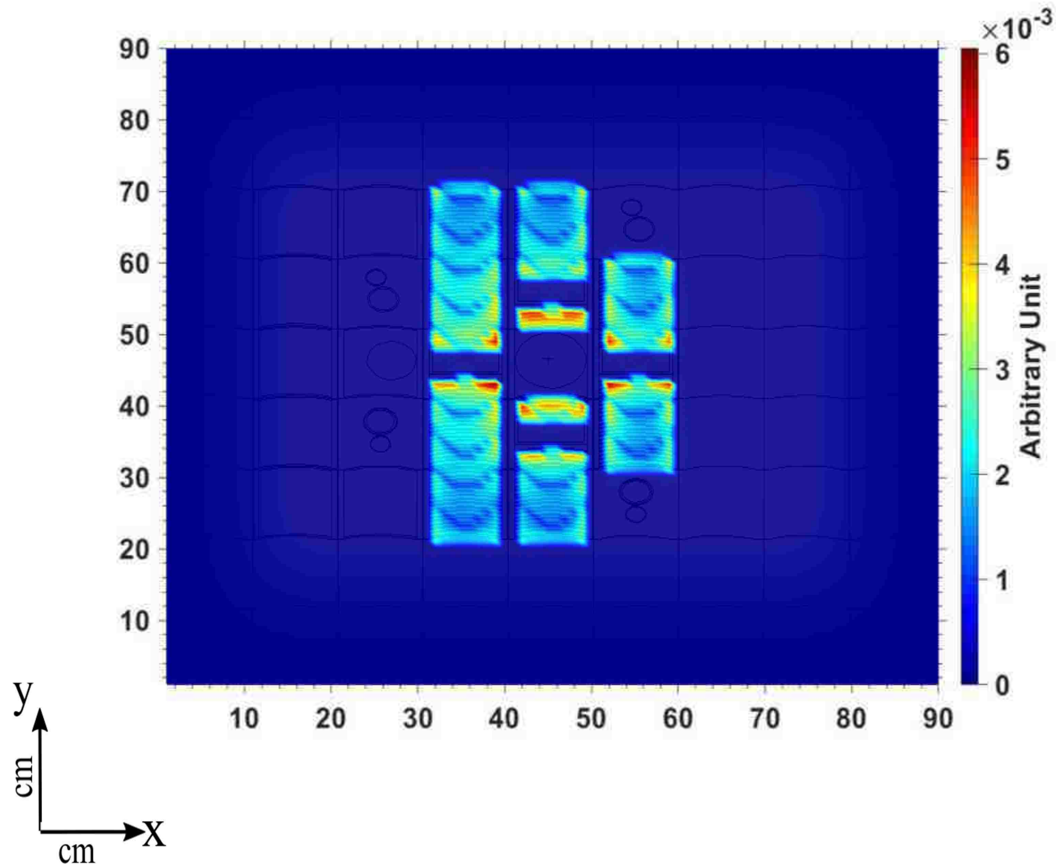

Figure 3.8. Hottest Fuel Plates for LPC Clean Core.

4. THE PROPOSED FLEXIBLE-POWER CONFIGURATION (FPC)

The goal of flexible-power configuration (FPC) is to combine the high flux levels of the HPC and multiple irradiation facilities in the LPC. FPC will operate at 2 MW and 200 KW. In the FPC configuration the disadvantage of both HPC and LPC will be eliminated. The disadvantage of the HPC was the limited number of irradiation facilities. The disadvantage of the LPC was the high concentration percentage of the required natural boron in control rod system for an effective safety shutdown. The FPC core considered the use of the same fuel type as of HPC and LPC core. For FPC core, the considered natural boron concentration for control rods system was 2%. This was the same percentage used for HPC core [28]. The included in-core irradiation facilities for FPC were FT, BRT, CRT, Hot Cell (HC) and two graphite-block irradiation facilities. The FT was positioned at the central region of the reactor core. HC facility was the same design as the FT facility. The design of BRT and CRT remain unchanged, same as the existing ones in the current MSTR core. The graphite-block irradiation facilities are like the design of BRT and CRT facilities but the element shell containing these facilities were filled with graphite [40]. These graphite-block irradiation facilities were labeled as BRT-GB and CRT-GB [40].

Figure 4.1 presented the core configuration for FPC. The proposed core configuration considered the compact core concept as of HPC core. The BeO/graphite composite reflector blocks surrounding the core determined to have 1 *cm* BeO thickness and 6.6 *cm* graphite thickness [41]. The determination of such thickness was adopted from previous study that optimized BeO to graphite thickness ratio for the composite reflector blocks for HPC core [41]. The core consists of four fuel elements, four control rods-fuel elements and six in-core irradiation facilities. The in-core irradiation facilities occupy the following positions E5, C6, G6, E3, D3, F3, see Figure 4.1.

	1	2	3	4	5	6	7	8	9
A									
B						GB			
C			GB	GB	GB	BRT	GB		
D		GB	BRT -GB	FE	CR1	FE	GB		
E		GB	HC	CR4	FT	CR3	GB		
F		GB	CRT -GB	FE	CR2	FE	GB		
G			GB	GB	GB	CRT	GB		
H						GB			
L									

GB: Graphite/BeO Composite Blocks FE: Fuel Element CR#: Control Rod
BRT: Bare Rabbit Tube CRT: Cadmium Rabbit Tube FT: Flux Trap
BRT-GB: BRT Inside GB CRT-GB: CRT Inside GB HC: Hot Cell

Figure 4.1. FPC Core Configuration.

4.1. MCNP MODEL AND SIMULATION CONDITIONS

MCNP6 was used for re-configuring the core for FPC [26]. The involved modification was repositioning the reactor core components as of Figure 4.1. A several tasks were identified for performing the simulation after incorporating all the necessary modifications for the MCNP model. These tasks were listed as the following:

1. Determination of neutron multiplication factor (k_{eff}).
2. Determination of control rods safety shutdown margin.
3. Determination of neutron flux map over the core and neutron flux spectrum in-core irradiation facilities.
4. Potential operational time comparison
5. Determination of hot-channel for clean core.

The number of particles per cycle, active cycles and total cycle were kept the same as these of previous configurations. As of previous configurations, same MCNP simulation conditions were applied for determining control rods worth, flux, hot-channel, and performing burnup calculation.

4.2. RESULTS AND DISCUSSION

This section included a calculation of k_{eff} and safety shutdown margin, determination of flux map and spectrum, evaluation of FPC potential operation time and determination of hot-channel.

4.2.1. Determination of k_{eff} and Comparison of Safety Shutdown Margin. The determination of k_{eff} was performed at room temperature with all control rods fully withdrawn along with the BeO/graphite composite reflector blocks surrounding the core. The determined k_{eff} was 1.02302 with an estimated standard deviation of 0.00038. An assumption has been made for two control rods to be the pair of shutdown control rods, the third control rod was the extra shutdown control rod and the fourth control rod was the regulating control rod. All the control rods positions for FPC core have been tested for the determination of optimum positions for the pair of shutdown control rods, extra shutdown control rod and the regulating control rod. The tests for shutdown control rods were based on the shutdown effectiveness (lower k_{eff}). Full insertion of CR1 and CR2 was determined to be the most effective pair control rods for shutdown. k_{eff} was determined to be 0.93390 with an estimated standard deviation of 0.00035. CR1 and CR2 occupies D5 and F5 positions respectively (see, Figure 4.1). CR4 and CR3 were assigned to be the extra shutdown control rod and the regulating rod, respectively. This results of positioning the control rods come in total agreement with the HPC core which due to the high similarity of both configuration [28, 41].

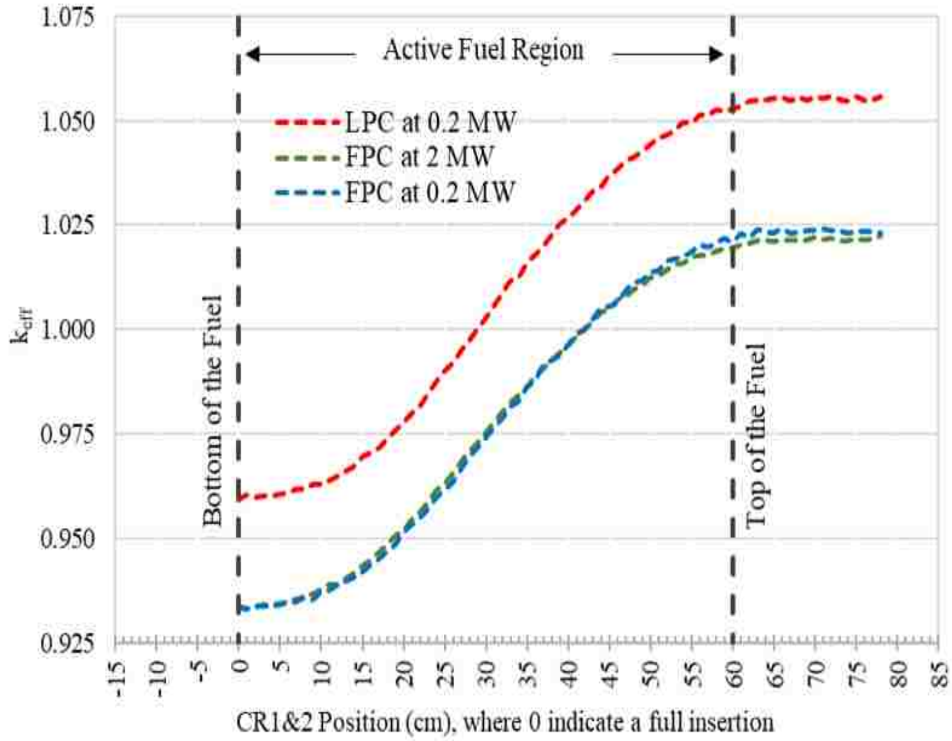

Figure 4.2. Comparison for the Worth of Paired Shutdown Control Rods (CR1&2).

A comparison for the worth of pair shutdown control rods is presented in Figure 4.2. With the FPC core configuration the core was effectively shutdown with 2% concentration of natural boron in control rod system at 2 MW and 200 KW. For previously proposed LPC core configuration, even with significant increase of the concentration of natural boron up to 12.6%, the shutdown is not effective as of FPC core [40]. The full insertion of CR1&2 for LPC bring k_{eff} to the point of 0.95910, see Figure 4.2 [40]. FPC core at 2 MW and 200 KW showed a better capability for control rod safety shutdown with only enhancing the boron concentration by 25% from the current MSTR core.

4.2.2. Neutron Flux Map and Capabilities. The neutron flux map for FPC core at 200 KW is illustrated in Figure 4.3. The highest neutron flux region is the middle region of the core which is the FT region. For FT facility, the total neutron flux calculated by MCNP at 200 KW was $1.42 \times 10^{13} \pm 1.78 \times 10^{11}$ $n\ cm^{-2}\ s^{-1}$. At 2 MW, the total neutron flux calculated was $1.42 \times 10^{14} \pm 1.78 \times 10^{12}$ $n\ cm^{-2}\ s^{-1}$. It should be noted that only the magnitude of flux is changing by one order of magnitude higher at 2 MW which is due to the change of power level. For the BRT and CRT, the total neutron flux calculated at 200 KW were $8.32 \times 10^{12} \pm 6.50{\times}10^{11}$ and $4.24 \times 10^{12} \pm 4.67 \times 10^{11}$ $n\ cm^{-2}\ s^{-1}$, respectively. At 2 MW, the total neutron flux calculated were $8.32 \times 10^{13} \pm 6.50{\times}10^{12}$ and $4.24 \times 10^{13} \pm 4.67 \times 10^{12}$ $n\ cm^{-2}\ s^{-1}$, respectively. For HC, BRT-GB and CRT-GB, the total neutron flux calculated at 200 KW were $8.14 \times 10^{12} \pm 1.71 \times 10^{11}$, $8.40 \times 10^{12} \pm 7.04 \times 10^{11}$ and $5.77 \times 10^{12} \pm 5.40 \times 10^{11}$ $n\ cm^{-2}\ s^{-1}$, respectively. At 2 MW, the total neutron flux calculated were $8.14 \times 10^{13} \pm 1.71 \times 10^{12}$, $8.40 \times 10^{13} \pm 7.04 \times 10^{12}$ and $5.77 \times 10^{13} \pm 5.40 \times 10^{12}$ $n\ cm^{-2}\ s^{-1}$, respectively. The flux level of FPC core at 2 MW is identical to the HPC flux level [28]. Also, the flux level of FPC core at 200 KW is identical to LPC flux level [40]. FPC prove its capability for combining both of flux level (for HPC and LPC) at a single flexible core.

Table 4.1 and Table 4.2 identified the contribution percentages of thermal, resonance and fast flux in each irradiation facilities at 200 KW and 2 MW, respectively. Also, the flux spectrum for all irradiation facilities of FPC core at 200 KW and 2 MW are presented in Figure 4.4, 4.5, 4.6 and 4.7, respectively. FT facility is the most suitable facility for fast neutron flux due to the 35.63% of the total produced flux in this facility was fast flux. Other facilities can be you used for fast flux are CRT-GB, BRT-GB and HC, see Table 4.1, Figure 4.4 and Figure 4.5. For thermal neutron flux, BRT facility is the most suitable facility due to the 50.15% of the total produced flux in this facility was thermal flux, see Table 4.1 and Table 4.2. Also, FT can be used for thermal flux as well as the rest of other facilities. For resonance flux, the two graphite-block irradiation facilities can be used along with the FT facility, see Table 4.2, Figure 4.6 and Figure 4.7.

The maximum total flux obtained in current MSTR core at 200 KW was reported to be $4.36 \times 10^{12} \pm 2.84 \times 10^{11}$ $n\ cm^{-2}\ s^{-1}$ at the BRT facility [12, 13, 42]. As flux comparison to FPC core with the same power-level, one order of magnitude higher was

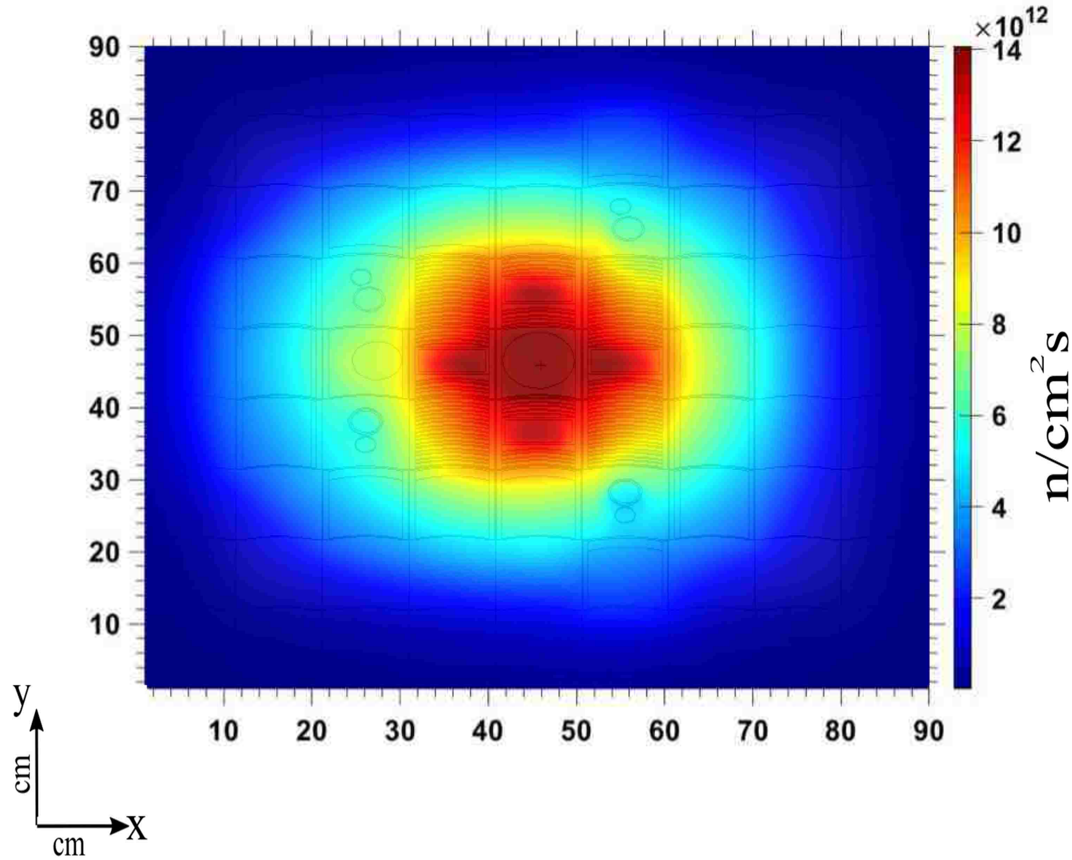

Figure 4.3. Neutron Flux Profile for FPC Core at 200 KW.

achieved. It should be noted that the current MSTR core configuration has nineteen bearing-fuel elements while FPC core configuration has only eight bearing-fuel elements (see, Figure 4.1). The advantages of the FPC core at 200 KW over the current MSTR core included; 1) lower load of fuel and 2) more irradiation facilities in core.

4.2.3. Comparison of Potential Operational Time. Figure 4.8 presented the potential operation time for FPC core compared to the previously proposed LPC and HPC core. For FPC, the burnup calculation was setup and performed using MCNP6. The goal is to determine how long the core can support criticality with an estimated operation temperature of 323.15 k for 200 KW core. The configured core for FPC supported 866 days (2.4 years) of continues operation with a critical core at 200 KW, see Figure 4.8. The initial k_{eff}

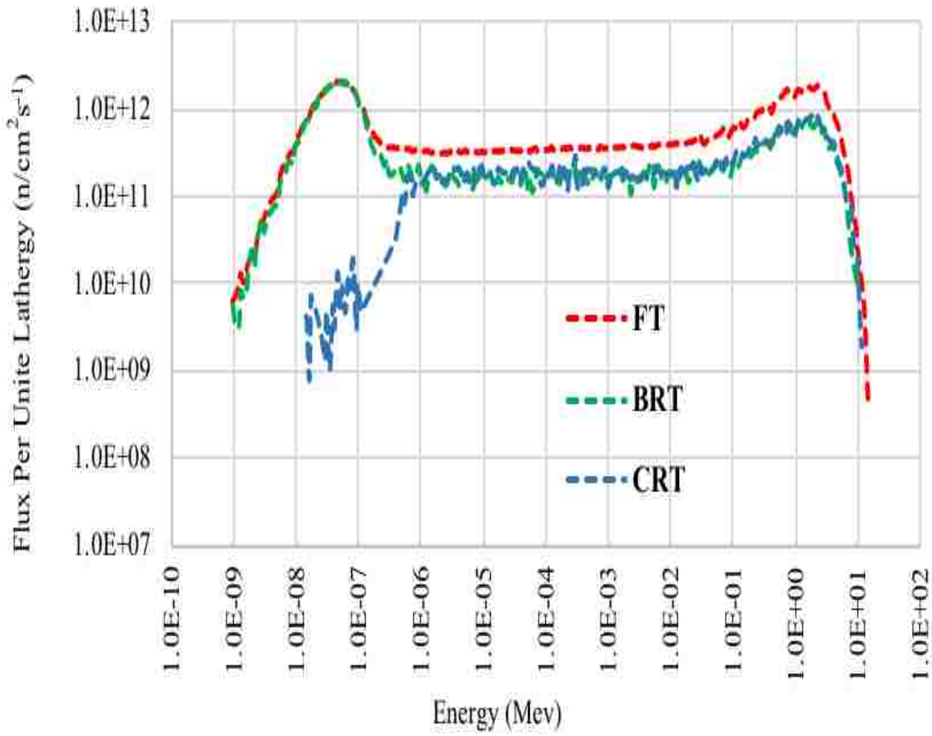

Figure 4.4. Neutron Flux Spectrum In-Core Irradiation Facilities-A for FPC at 200 KW.

started at 1. 02334 (at zero-time step) with an estimated standard deviation of 0.00036. By 867 days of operating at 200 KW, k_{eff} dropped to 0.99971 (subcritical) with an estimated standard deviation of 0.00037. LPC core with an estimated operation temperature of 323.15 k and power level of 200 KW can critically operate for more than 2010 days (~ 5 years and 5 months), see Figure 4.8. By the day of 2010, k_{eff} was 1.02882 with an estimated standard deviation of 0.00034. MCNP simulation was terminated after 2010 days of operation, assuming no further operation time is needed. The LPC core has higher fuel load by 64% than the FPC core. HPC core with an estimated operation temperature of 341.12 k and power level of 2 MW, can critically operate for two months (61 days), see Figure 4.8. By 62 days, the HPC core went subcritical. FPC core with an estimated operation temperature of

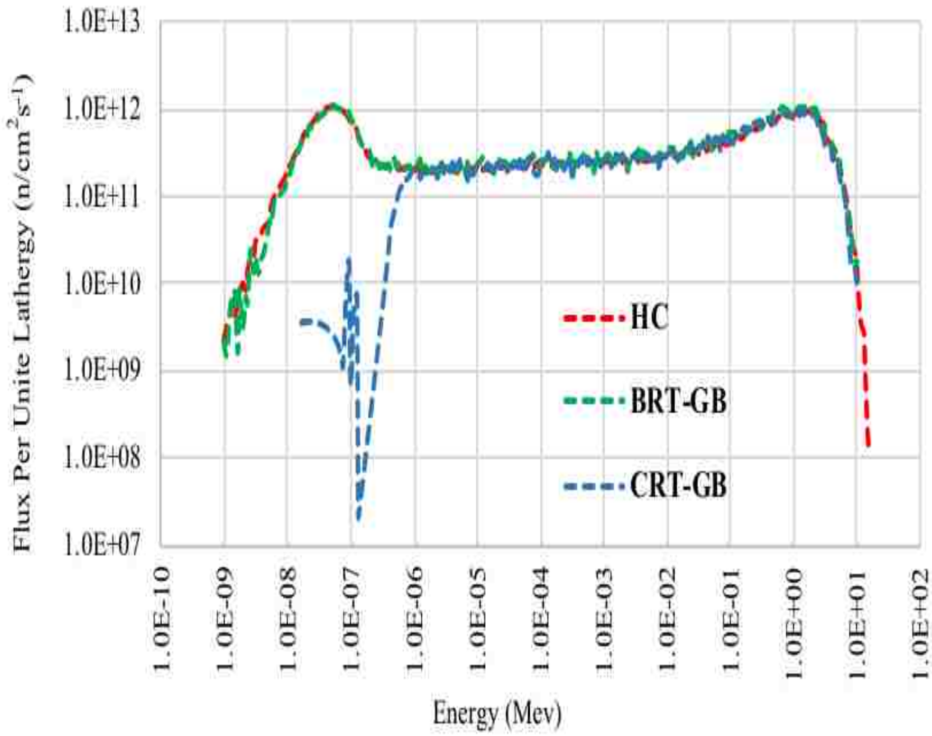

Figure 4.5. Neutron Flux Spectrum In-Core Irradiation Facilities-B for FPC at 200 KW.

341.12 K and power level of 2 MW, can critically operate for 2.25 days (54 hours). At 200 KW, both LPC and FPC can operate for long period of time. However, FPC core provided the needed flexibility in operation time with less load of fuel.

4.2.4. Determination of Hot-Channel. The hot-channel for FPC clean core (fresh fuel and zero burnup) was determined using MCNP6. The core contains a total of 112 fuel plates. Assuming clean core for FPC at 2 MW, the fission energy deposition is plotted in Figure 4.9. Considering the illustration figure for the sequence of fuel plates in each fuel element "Figure 2.8". The hottest fuel plate among the FPC core was determined to be in control rods number 2 (CR2 occupied position F5, see Figure 4.1). Fuel plate number 1 (FP#1) was the hottest fuel plate. It's adjacent to the most-outer water channel. FP#1 was the highest calculated power distribution among other fuel plates in core. The calculated power distribution for FP#1 was 32.2 kW. FP#1 contributed 1.61% of the total

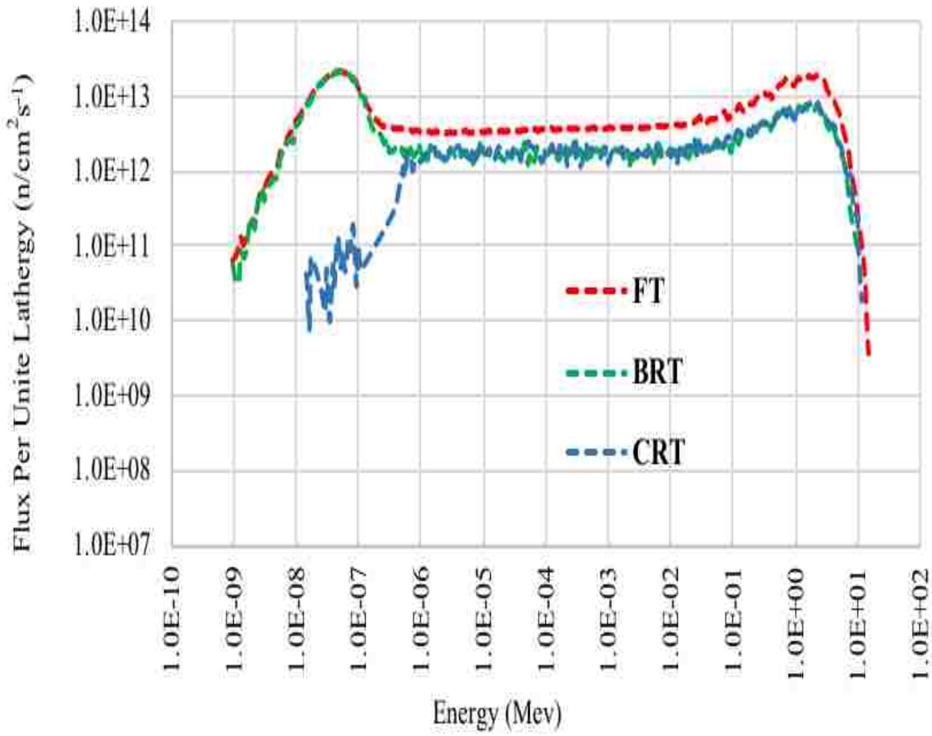

Figure 4.6. Neutron Flux Spectrum In-Core Irradiation Facilities-A for FPC at 2 MW.

power distribution. The variation of power distribution among the width and the length of FP#1 is due to the increase of local water-to-fuel ratio in these regions. For clean core of FPC, the hot-channel is located between FP#1 and FP#2 of CR2. In FPC clean and core at 2 MW, the depletion rate of control rods' fuel plates is higher than the average fuel plates. Rotating the four control rods by 90 degree can mitigate the reactivity effect. However, after long operation time, replacing control rod-fuel elements will be necessary. The total produced power by the hottest fuel plate of FPC core at 2 MW is less by 225.86 W compared to the total produced power by the hottest fuel plate of HPC core at 2 MW [41]. Thus, the generated heat should be safely transfere and remove without exceeding the safety limits as proven by the CFD modeling for HPC core, see section 2.

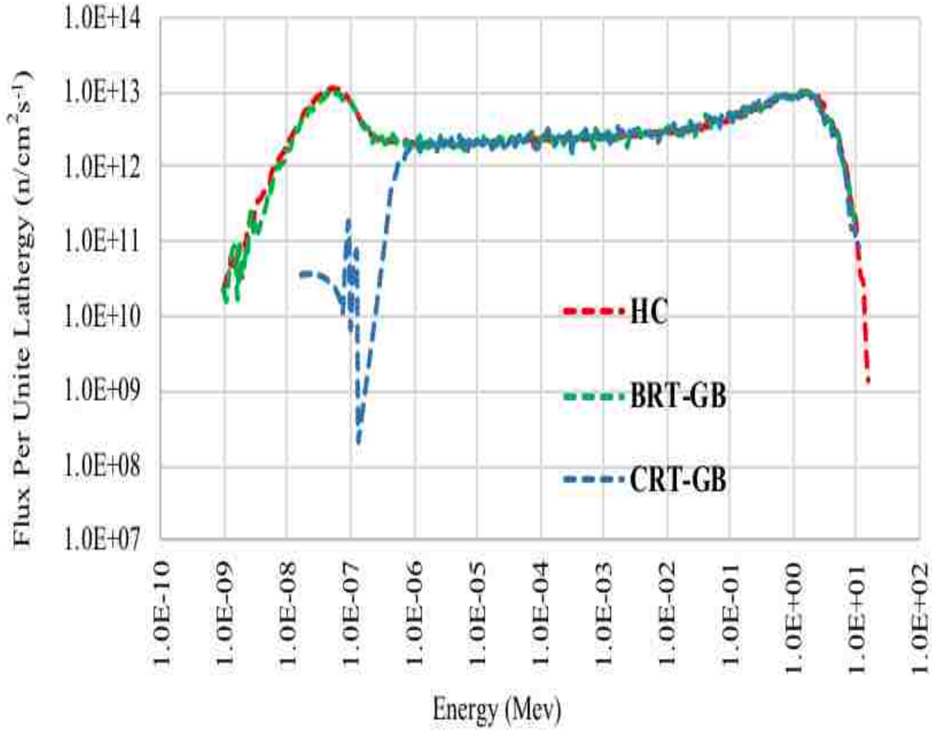

Figure 4.7. Neutron Flux Spectrum In-Core Irradiation Facilities-B for FPC at 2 MW.

Table 4.1. Neutron Flux Spectrum In-Core Irradiation Facilities for FPC at 200 KW.

	FT		BRT		CRT	
Thermal	4.57E+12	32.14%	4.17E+12	50.15%	3.01E+10	0.71%
Resonance	4.59E+12	32.23%	2.18E+12	26.24%	2.18E+12	51.35%
Fast	5.07E+12	35.63%	1.97E+12	23.62%	2.03E+12	47.94%
Total	1.42E+13	100.00%	8.32E+12	100.00%	4.24E+12	100.00%
	HC		BRT-GB		CRT-GB	
Thermal	2.34E+12	28.82%	2.22E+12	26.40%	2.36E+10	0.41%
Resonance	3.02E+12	37.10%	3.23E+12	38.49%	3.05E+12	52.80%
Fast	2.77E+12	34.08%	2.95E+12	35.11%	2.70E+12	46.79%
Total	8.14E+12	100.00%	8.40E+12	100.00%	5.77E+12	100.00%

Table 4.2. Neutron Flux Spectrum In-Core Irradiation Facilities for FPC at 2 MW.

	FT		BRT		CRT	
Thermal	4.57E+13	32.14%	4.17E+13	50.15%	3.01E+11	0.71%
Resonance	4.59E+13	32.23%	2.18E+13	26.24%	2.18E+13	51.35%
Fast	5.07E+13	35.63%	1.97E+13	23.62%	2.03E+13	47.94%
Total	1.42E+14	100.00%	8.32E+13	100.00%	4.24E+13	100.00%
	HC		BRT-GB		CRT-GB	
Thermal	2.34E+13	28.82%	2.22E+13	26.40%	2.36E+11	0.41%
Resonance	3.02E+13	37.10%	3.23E+13	38.49%	3.05E+13	52.80%
Fast	2.77E+13	34.08%	2.95E+13	35.11%	2.70E+13	46.79%
Total	8.14E+13	100.00%	8.40E+13	100.00%	5.77E+13	100.00%

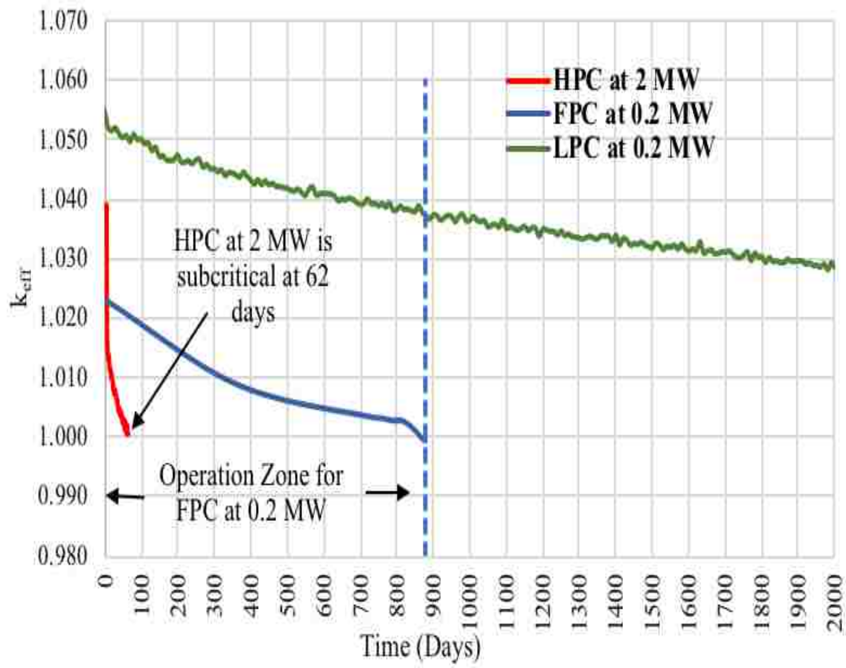

Figure 4.8. Comparison of Potential Operation Time.

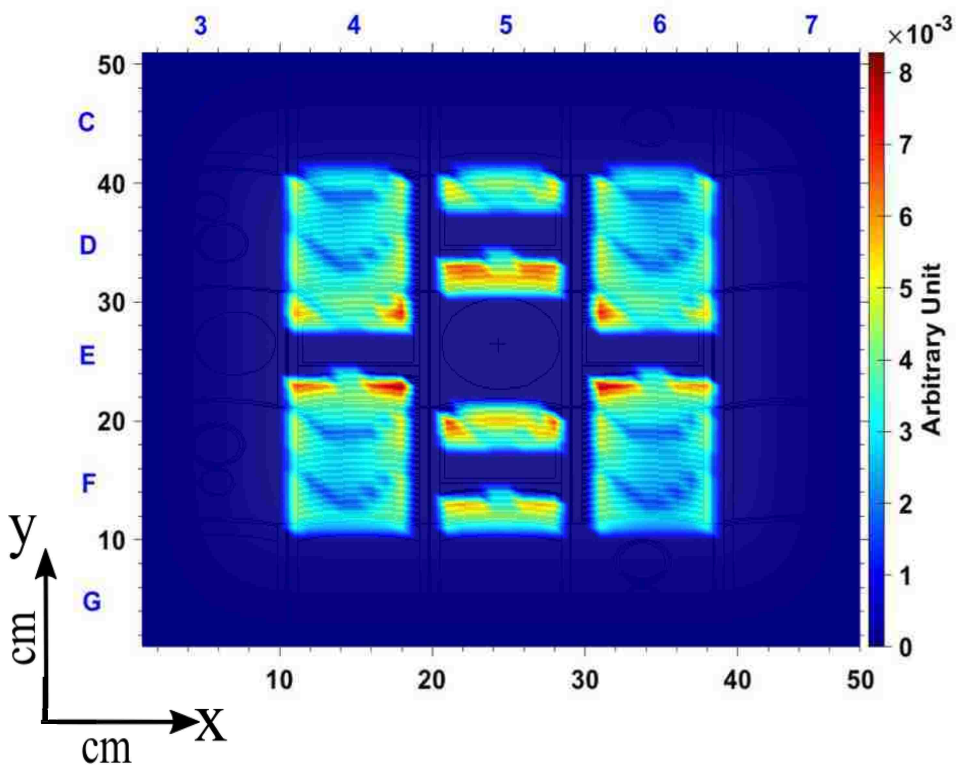

Figure 4.9. Hottest Fuel Plates for FPC Clean Core at 2 MW (C-G and 3-7 grid reference labels; blue colored).

5. CONCLUSIONS

The goal of this research was achieved. The goal was to overcome the attendant rigidity of the traditional design of research reactor and provide adaptability and flexibility in supporting a wide variety of advance experiments and research. A reactor core was designed and configured for allowing multi-spectral capability. The fuel and control rods system geometries were adopted from MSTR. The adopted fuel was U-10Mo fuel with a physical density of 16.09 g/cm3 and 19.75% U-235 enriched. This is because of its high uranium density, stability and predictable irradiation behavior. The configurations adopted compact core concept (core surrounded with reflector blocks) along with the flux trap (FT) facility at the center region of the core. This allowed the concentration of neutron flux at the center of the core. Two power-levels were considered: high-power configuration (HPC) at 2 MW and low-power configuration (LPC) at 200 KW. Flexible-power configuration (FPC) that can operate at 2 MW and 200 KW was adopted to combin the advantages of both HPC and LPC configurations. For each of the proposed configurations, the conclusion remarks are described in the following sections:

5.1. HIGH-POWER CONFIGURATION (HPC)

The goal of HPC core was to achieved high flux capability for advance experiments and researches. The proposed core for HPC included four fuel elements, four partial fuel elements with control rod access, four control rods, three in-core irradiation facilities and BeO/graphite composite reflector blocks surrounded the core. The k_{eff} for HPC core was evaluated at room temperature with all control rods fully withdrawn. The core sustain criticality with a determined k_{eff} of 1.03853, which is within the 4.5% delta-k/k constraint on excess reactivity. This was made possible by using BeO/graphite composite reflector blocks with 1cm BeO thickness. The boron concentration in steel control rods system was increased from 1.5% to 2% in order to attain effective shutdown. It was necessary to pair control rods 1 and 2 in order to achieve adequate shutdown margin. A backup control rods provided additional safety measure in shutdown conditions.

The total neutron flux calculated by MCNP were $1.42\times10^{14} \pm 1.78\times10^{12}$, $8.23\times10^{13} \pm 6.48\times10^{12}$ and $4.15\times10^{13} \pm 4.63\times10^{12}$ $n\ cm^{-2}\ s^{-1}$ in FT, BRT and CRT respectively. Based on the energy spectrum and flux magnitude for specific irradiation locations, the most suitable facility for fast, resonance and thermal flux were FT, CRT and BRT respectively. The maximum flux in HPC core was two orders of magnitude higher than the maximum obtainable in current MSTR core configuration. This demonstrates the potential flux enhancement achievable in HPC core. Additionally, HPC's flux capability was similar in magnitude to the current flux capabilities of the 6 MW MITR research reactor "1.2×10^{14}". With the composite reflector blocks in place, the HPC could sustain continuous operation at 2 MW power level for two months. This will allow longer time for performing experiments and research between refueling. The hot-channel for both clean and burned core was located between FP#14 and FP#15 of the backup control rod (CR4). Also, larger fractions of power were produced in the fuel elements with control rod channel. Hence, these elements would have to be replaced more frequently due to their faster depletion rate.

A representational 3D model containing HPC's two fuel plate with a single coolant-channel in between was simulated using ANSYS Fluent. By applying the maximum generated heat by the hottest fuel plates along with an assumption of high coolant inlet temperature, the simulated model of HPC didn't exceed the safety limits. Safety limits included water boiling point at 178.8 KPa, melting point for U-10Mo and clad (6061 Al) along with the delamination limit for U-10Mo plate-type fuel. At full operation power of HPC core, the mass flow rate of 39.86 kg/s (10.644 gallon/s) was sufficient for removing the generated heat. An average pumping system in current market can produce such requirement. However, a pumping system with higher capability can add an extra safety assurance.

5.2. LOW-POWER CONFIGURATION (LPC)

The goal of LPC was to enhance the reactor by the inclusion of additional irradiation facilities for core robustness in supporting multiple tests at a time. The initial core configuration for LPC was like the HPC configuration but with additional three in-core irradiation facilities and graphite reflector blocks surrounding the core. This resulted in low k_{eff} value. Thus, LPC adopted extra fuel load in order to improve the low value of k_{eff}. The proposed LPC core consisted of eight fuel elements, four control rods and six in-core irradiation facilities. The concentration of natural boron in control rod system was increased to 12.6% in order to allow for an effective safety shutdown. The core sustain criticality with a determined k_{eff} of 1.05568. Pair of shutdown control rods (CR1&2) were effectively able to shutdown the core with a determined k_{eff} of 0.95910.

At 0.2 MW, the total neutron flux calculated by MCNP at FT, BRT and CRT were $1.03 \times 10^{13} \pm 1.52 \times 10^{11}$, $6.42 \times 10^{12} \pm 5.72 \times 10^{11}$ and $3.28 \times 10^{12} \pm 4.07 \times 10^{11}$ $n\ cm^2\ s^{-1}$, respectively. For graphite-block irradiation facilities (FT-GB, BRT-GB and CRT-GB) the total neutron flux calculated by MCNP were $6.54 \times 10^{12} \pm 1.53 \times 10^{11}$, $7.02 \times 10^{12} \pm 6.45 \times 10^{11}$ and $4.93 \times 10^{12} \pm 4.94 \times 10^{11}$ $n\ cm^2\ s^{-1}$, respectively. Based on the flux magnitude and spectrum for each irradiation facilities, the most suitable facility for fast, resonance and thermal flux were FT, graphite-block irradiation facilities and BRT, respectively. Maximum achieved flux at FT facility of LPC core was higher by one ordered of magnitude compared to the current MSTR core configuration. hot-channel was located between fuel plate number 14 and 15 of the control rod number 4 (CR4).

5.3. FLEXIBLE-POWER CONFIGURATION (FPC)

The goal of FPC was to combine the high flux levels of the HPC and multiple irradiation facilities in the LPC with a single core. The FPC core consist of four fuel elements, four control rods-fuel elements, six in-core irradiation facilities and surrounded from all sides by BeO/graphite composite reflector blocks. The adopted thickness for BeO was 1 *cm* and 6.6 *cm* for graphite in the composite reflector blocks as optimized by HPC core. The six included irradiation facilities were FT, BRT, CRT, HC, BRT-GB and CRT-GB. The k_{eff} for the proposed core was evaluated at room temperature with all control rod fully with drawn. The determined k_{eff} was 1.02302 with estimated standard deviation of 0.00038. The concentration of natural boron in the control rod system was 2% similar to the HPC core. With the full insertion of the pair of shutdown control rods (CR1&2), k_{eff} was 0.93390. An effective safety shutdown was achieved for FPC core. At 2 MW, FPC core was able to sustain criticality for a continues operation of 2.25 days (54 hours). At 200 KW, core was able to criticality operate for 2.4 years. FPC allowed for a reasonable operation time at low-power level which support sufficient time for experiments and researches.

For FT facility, the total neutron flux calculated by MCNP at 2 MW and 200 KW were $1.42 \times 10^{14} \pm 1.78 \times 10^{12}$ and $1.42 \times 10^{13} \pm 1.78 \times 10^{11}$ $n\ cm^{-2}\ s^{-1}$, respectively. For the BRT and CRT, the total neutron flux calculated at 200 KW were $8.32 \times 10^{12} \pm 6.50 \times 10^{11}$ and $4.24 \times 10^{12} \pm 4.67 \times 10^{11}$ $n\ cm^{-2}\ s^{-1}$, respectively. At 2 MW, the total neutron flux calculated were $8.32 \times 10^{13} \pm 6.50 \times 10^{12}$ and $4.24 \times 10^{13} \pm 4.67 \times 10^{12}$ $n\ cm^{-2}\ s^{-1}$, respectively. For HC, BRT-GB and CRT-GB, the total neutron flux calculated at 200 KW were $8.14 \times 10^{12} \pm 1.71 \times 10^{11}$, $8.40 \times 10^{12} \pm 7.04 \times 10^{11}$ and $5.77 \times 10^{12} \pm 5.40 \times 10^{11}$ $n\ cm^{-2}\ s^{-1}$, respectively. At 2 MW, the total neutron flux calculated were $8.14 \times 10^{13} \pm 1.71 \times 10^{12}$, $8.40 \times 10^{13} \pm 7.04 \times 10^{12}$ and $5.77 \times 10^{13} \pm 5.40 \times 10^{12}$ $n\ cm^{-2}\ s^{-1}$, respectively. The flux level of FPC core at 2 MW and 200 KW was identical to the HPC and LPC flux level, respectively. Based on the flux magnitude and spectrum for each irradiation facilities, the most suitable facility for fast, thermal and resonance flux were FT, BRT and graphite-block irradiation facilities, respectively. The advantages of the FPC core over the LPC core included lower load of fissile fuel. The advantages of the FPC core over the HPC core included multiple irradiation facilities. For clean core of FPC, the hot-channel was determined between FP#1 and FP#2 of CR2. Control rods-fuel elements have to be replaced frequently due to their faster depletion rate. The total produced power by the FPCs' hottest fuel plate was less by 225.86 W compared to HPC core. Thus, without exceeding the safety limits, the generated heat was assumed to be safely transferred and removed.

APPENDIX

MCNP AND CFD MODELS

1. MCNP MODELS

Any inquiries about the MCNP model for HPC, LPC and FPC should be directed to Thaqal Alhuzaymi at tatzd@mst.edu or thaqal@hotmail.com.

2. CFD MODEL

Any inquiries about the CFD model should be directed to Thaqal Alhuzaymi at tatzd@mst.edu or thaqal@hotmail.com.

REFERENCES

[1] Eric Christopher Forrest. *Study of turbulent single-phase heat transfer and onset of nucleate boiling in high aspect ratio mini-channels to support the MITR LEU conversion*. PhD thesis, Massachusetts Institute of Technology, Doctoral Dissertations, 2014.

[2] *Applications of Research Reactors*. Number NP-T-F.3 in Nuclear Energy Series. INTERNATIONAL ATOMIC ENERGY AGENCY, Vienna, 2014.

[3] Utilization related design features of research reactors: A compendium. Technical Report 455, Vienna, 2009.

[4] JL Marshall. Fast flux test facility (fftf) maintenance provisions. Technical report, Hanford Engineering Development Lab., Richland, WA (USA), 1981.

[5] Sidney Drell, David Hammer, JM Cornwall, F Dyson, and R Garwin. Use of the fast flux test facility for tritium production. Technical report, MITRE CORP MCLEAN VA JASON PROGRAM OFFICE, Virginia 22102-3481., 1996.

[6] Oak Ridge National Laboratory (ORNL). High flux isotope reactor (hfir) user guide, revision 2.0, tn 37831, November 2015.

[7] Clifford J Stanley and Frances M Marshall. Advanced test reactor: A national scientific user facility. In *16th International Conference on Nuclear Engineering*, pages 367–372. American Society of Mechanical Engineers Digital Collection, 2009.

[8] International Atomic Energy Agency (IAEA). IAEA's research reactors database, 2018.

[9] Douglas Morrell. Annual report research reactor infrastructure program. Technical report, Idaho National Laboratory (INL)INL/EXT-12-27816, 2012.

[10] University of missouri, columbia missouri university research reactor. *LICENSE RENEWAL APPLICATION SAFETY ANALYSIS REPORT*, 1, 2006.

[11] K Sun, L Hu, E Wilson A Bergeron, and T Heltemes. Low enriched uranium (leu) conversion preliminary safety analysis report for the mit research reactor (mitr). Technical report, Massachusetts Institute of Technology (MIT). , Cambridge, Massachusetts., 2017.

[12] Meshari ALQahtani and Ayodeji B Alajo. Characterization of prompt neutron spectrum of the missouri university of science and technology reactor. *Nuclear Engineering and Design*, 320:57–64, 2017.

[13] W Bonzer and C Carroll. Safety analysis report for the missouri university of science and technology reactor-revision 2. *Rolla, MO*, 2008.

[14] Isaac John Bratton. *Modeling and Validation of the Fuel Depletion and Burnup of the OSU Research Reactor Using MCNPX/CINDER'90*. PhD thesis, The Ohio State University, Columbus, OH USA 43210., 2012.

[15] C. H. Townsend. Technical specifications for the purdue university reactor, pur-1. docket number 50-180. Technical report, West Lafayette, IN 47907, 2016.

[16] University of Massachusetts Lowell (UMASS). Safety analysis report- university of massachusetts lowell research reactor (umlrr). chapter 1-7. Technical report, License R-125. Docket 50-223. 2015 Rev.0, 2015.

[17] EH Wilson, A Bergeron, JA Stillman, TA Heltemes, D Jaluvka, and L Jamison. Us high performance research reactor conversion program: An overview on element design. In *European Research Reactor Conference*, Rotterdam, Netherlands, 2017.

[18] RG Muranaka. Conversion of research reactors to low-enrichment uranium fuels. *IAEA Bulletin*, 25(1):18–20, 1983.

[19] Department of Energy (DOE), National Nuclear Security Administration. 2019. Material Management and Minimization (3M). https://nnsa.energy.gov/aboutus/ourprograms/dnn/m3.

[20] Ahmadu Bello University (ABU), March 2019. ABU News. Main Campus, Samaru, Zaria. ISSN:0345-0749. Vol. 6 No. 1. https://www.abu.edu.ng/news-and-events/news/magazines/files/abunews-march-2019.pdf.

[21] Nuclear Regulatory Commission et al. Safety evaluation report related to the evaluation of low-enriched uranium silicide-aluminum dispersion fuel for use in non-power reactors. Technical report, Nuclear Regulatory Commission, 1988.

[22] Mitchell K Meyer. Investigation of the cause of low blister threshold temperatures in the rertr-12 and afip-4 experiments. Technical report, Idaho National Laboratory (INL), 2012.

[23] A Bergeron, EH Wilson, G Yesilyurt, FD Dunn, JG Stevens, L Hu, and TH Newson Jr. Low enriched uranium core design for the massachusetts institute of technology reactor (mitr) with un-finned 12 mil-thick clad umo monolithic fuel. Technical report, Argonne National Lab.(ANL), Argonne, IL (United States), 2013.

[24] J Stillman, E Feldman, L Foyto, K Kutikkad, JC McKibben, N Peters, and J Stevens. Technical basis in support of the conversion of the university of missouri research reactor (murr) core from highly-enriched to low-enriched uranium-core neutron physics. Technical report, Argonne National Lab.(ANL), Argonne, IL (United States),ANL/RERTR/TM-12-30, 2012.

[25] Leland M Montierth. Criticality safety evaluation for the advanced test reactor enhanced low enriched uranium fuel elements. Technical report, Idaho National Lab.(INL), Idaho Falls, ID (United States),INL/EXT-16-39590, ECAR-2371, Revision: 1., 2016.

[26] Christopher J Werner et al. Mcnp users manual-code version 6.2. *Los Alamos National Laboratory, LA-UR-17-29981*, 2017.

[27] November ANSYS. Ansys fluent in ansys workbench user's guide. ansys. *Inc., Release*, 15, 2013.

[28] Thaqal Alhuzaymi and Ayodeji Babatunde Alajo. Achieving high-power configuration in Missouri S&T Reactor (MSTR) for potential uprate. 2019.

[29] U.S. Geological Survey. Metal prices in the united states through 2010. Technical Report 2012–5188, U.S. Geological Survey Scientific Investigations Report, 2013. [Online; accessed 25-October-2019].

[30] Klaus J Schulz, John H DeYoung, Robert R Seal, and Dwight C Bradley. *Critical Mineral Resources of the United States: Economic and Environmental Geology and Prospects for Future Supply*. Geological Survey, 2017. [Online; accessed 25-October-2019].

[31] M Albarhoum. Reactivity cost for different top reflector materials in miniature neutron source reactors. *Progress in Nuclear Energy*, 58:39–44, 2012.

[32] S Dawahra, K Khattab, and G Saba. Investigation of BeO as a reflector for the low power research reactor. *Progress in Nuclear Energy*, 81:1–5, 2015.

[33] S Dawahra, K Khattab, and G Saba. Study the effects of different reflector types on the neutronic parameters of the 10 mw mtr reactor using the mcnp4c code. *Annals of Nuclear Energy*, 85:1115–1118, 2015.

[34] Farrokh Khoshahval and Farhad Salari. Sensitivity analyses of the use of different reflector materials on the neutronics parameters of tehran research reactor. *Progress in Nuclear Energy*, 93:351–361, 2016.

[35] Jiwei Wang. *Developing a high thermal conductivity nuclear fuel with silicon carbide additives*. University of Florida, 2008.

[36] Kelly Christopher Rogers O'Bryant. Hot channel determination and burnup analysis of missouri university of science and technology research nuclear reactor. 2012.

[37] Daxin Gong, Shanfang Huang, Guanbo Wang, and Kan Wang. Heat transfer calculation on plate-type fuel assembly of high flux research reactor. *Science and Technology of Nuclear Installations*, 2015, 2015.

[38] AB Robinson, GS Chang, DD Keiser Jr, DM Wachs, and DL Porter. Irradiation performance of u-mo alloy based 'monolithic'plate-type fuel–design selection. Technical report, Idaho National Laboratory (INL), 2009.

[39] Lester Haar, John S Gallagher, and George S Kell. Steam tables: Thermodynamic and transport properties and computer programs for vapor and liquid states of water in si units. In *NBS/NRC—National Standard Reference Data System*, page 320. Hemisphere New York, NY, 1984.

[40] Thaqal Alhuzaymi and Ayodeji Babatunde Alajo. Low-power core reconfiguration for Missouri S&T Reactor (MSTR). 2019.

[41] Ayodeji B. Alajo Thaqal Alhuzaymi. Hot-channel and burnup analysis for potential high-power configuration of Missouri S&T Reactor . ANS Winter Meeting 2019, American Nuclear Society., 2019.

[42] B Richardson, Carlos H Castano, J King, A Alajo, and Shoaib Usman. Modeling and validation of approach to criticality and axial flux profile experiments at the Missouri S&T Reactor (MSTR). *Nuclear Engineering and Design*, 245:55–61, 2012.

VITA

Thaqal Alhuzaymi was born in the town of Aljimsh in Riyadh province, Saudi Arabia. By 2005, Thaqal earned a scholarship from the King Abdullah Scholarship Program (KASP) to study abroad. In December 2009, he received his Bachelor of Science degree in System Engineering from the University of Arkansas at Little Rock (UALR), USA. At an academic researcher position at the Nuclear Sciences Research Institute (NSRI), he joined the King Abdulaziz City of Sciences and Technology (KACST) in 2010. By January 2012, Thaqal was awarded a graduate scholarship and joined the Missouri University of Science and Technology (Missouri S&T). He received his Master of Science degree in Nuclear Engineering by 2013 and continued his Ph.D. studies under the supervision of Dr. Ayodeji B. Alajo. During the first four years, Thaqal's Ph.D. studies involved developing a safeguard and nonproliferation framework applicable to developing states in the Middle East and North Africa (MENA) region. During this time, Thaqal joined Brookhaven National Laboratory (BNL) for a summer internship course in nuclear nonproliferation, security, and safeguards. Thaqal published four peer-reviewed papers on the topic of safeguards in the Journal of Nuclear Material Management (JNMM), the Institute of Nuclear Material Management (INMM), and the American Nuclear Society (ANS). By 2017, Thaqal shifted his Ph.D. studies to reactor design and analysis. The goal of this new topic was the design of a research reactor with multi-spectral capability. He has published three peer-reviewed papers on the topic of reactor design, while three additional papers are currently under review. Thaqal was a member of several nuclear organizations, including INMM, ANS and the World Institute for Nuclear Security (WINS). In December 2019, Thaqal received a Doctor of Philosophy degree (Ph.D.) in Nuclear Engineering from Missouri S&T.